A review of principles and options for the re-use of machining chips by solid, semi-solid or melt-based processing

James W. Murray[1*], Xiaoliang Jin[4], Christopher J. Cleaver[2], Jose M.C. Azevedo[2], Zhirong Liao[1], Wenbin Zhou[3], Jonathan M. Cullen[2], Julian M. Allwood[2], Adam T. Clare[1]

[1]Department of Mechanical, Materials and Manufacturing Engineering, Faculty of Engineering, University of Nottingham, Nottingham, NG7 2RD, UK

[2]Department of Engineering, University of Cambridge, Cambridge, CB2 1PZ, UK

[3]Department of Mechanical Engineering, Imperial College London, London, SW7 2AZ, UK

[4]Department of Mechanical Engineering, The University of British Columbia, Vancouver, V6T 1Z4, Canada

*Corresponding author email: james.murray@nottingham.ac.uk, tel. +447816189239

Abstract

Machining chips are a potentially versatile material feedstock to be used in a range of solid-state and melt based manufacturing processes. The poor current understanding of the behaviour of chips in such processes limits the likelihood of practical adoption of such materials on an industrial scale. The re-use (as opposed to recycling or landfilling) of machining waste offers both economic and environmental savings. Iron and steel production causes up to 9%, and aluminium up to 1.5% of global process and energy CO_2 emissions. It is proposed that between 0.24% and 0.5% (117 Mt CO_2) of global CO_2 emissions could be saved by reusing steel machining chips and between 0.13% and 0.22% (51 Mt CO_2) via re-use of aluminium chips, through mitigation of recycling associated emissions or emissions from generation of new steel. Re-use of large manufacturing scrap, i.e. the majority of such scrap, increases these values to savings of 1% and 0.86% of global CO_2 emissions for steel and aluminium respectively in the best scenario. This work gives a perspective on the potential for chips to retain value and be re-used in manufacturing process streams. The paper guides the reader from the generation and control of machining chips, to the principles of material consolidation. The principles of material densification by both solid state and laser deposition based methods are described, and current and potential manufacturing processes which can use chips as a feedstock are critically reviewed in terms of their practicalities and final properties. A perspective on potential CO_2 savings is described, providing the underpinning motivation behind this work. It is shown there is significant potential for versatile manufacturing using machining chips by both solid-state and laser-based processing of chips into finished products. An argument is also presented for a new approach to processing large-scrap, e.g. from the automotive manufacturing industry, as well as end-of-life automotive scrap, into smaller chips ready for re-use.

Keywords: CO_2; machining chips; re-use; steel; aluminium

1. Introduction

Mechanical machining, in particularly turning, milling and drilling, are essential processes in the manufacturing sector, and are critical to the creation of both simple and complex shaped components

and products from metals. Mechanical machining by definition creates machining chips, which are typically generated under application of a coolant to the machining area. Machining waste generated by machining shops or manufacturing plants are likely to be mixed with other materials which have been machined using the same tool, and contaminated with coolant residue and other species from the surroundings. A realistic approach for dealing with this waste material is either selling to a scrap collector, who will likely recycle it, or disposing directly to landfill. The principle of direct re-use as opposed to recycling and landfilling offers both economic and environmental advantages, particularly in the case of steel as well as aluminium. In this paper, the term 're-use' specifically refers to the direct use of machined chips for the subsequent manufacturing process to fabricate final or near-net-shape parts. In contrast, 'recycling' refers to the traditional method of recycling machined chips through compacting, remelting, casting, homogenizing, sawing, and extrusion, with the extruded parts serving as billets to be further manufactured into the final products [1]. In global manufacturing processes, machining chips constitute 14.6% of waste for steel and 13.7% for aluminium [2]. Iron and steel production is responsible for up to 9% of global process and energy CO_2 emissions [3–5]. Process and energy emissions account for 64% of anthropogenic CO_2 emissions [6,7], the rest being attributed to deforestation, agriculture and decay. Globally, we produce 24 times less aluminium than steel [8]. Despite this, aluminium accounts for 1% [2, 8] – 1.5% [9] of CO_2 emissions given its high primary production energy requirements.

Manufacturing with iron and steel can generate a significant amount of scrap waste in the form of machining chips. According to the 'Steel Scrap - Global Strategic Business Report' [10], the global market for steel scrap was estimated at 529.2 million tons in 2023 and is projected to reach 738 million tons by 2030. Machining chips account for a significant portion of this steel scrap [11]. Much of the chips are recycled, though some are disposed of in landfills. Recycling of this material somewhat mitigates some of the CO_2 emissions associated with iron and steel production, as 1) blast furnaces are not required in this process, avoiding direct CO_2 emissions from coke usage, and 2) less energy is required per kg to produce recycled iron and steel than primary steel. However, the sheer volume of iron and steel which is produced and required, means 1% of global emissions of CO_2 arise from remelting of scrap [12]. Hence, there is an emission-based incentive to avoid remelting such waste, and instead we must look to ways to directly re-use it. In addition, re-purposed material has the potential to replace material which would otherwise be produced from iron ore, and hence emissions savings greater than 1% of global contributions are possible.

This work gives a perspective on chip re-use from the generation and control of machining chips, to current and potential re-use methods. The choice of the manufacturing sector to replace conventional feedstocks with machining chips relies on both an effective understanding of the principles of material densification as well as the expected properties of parts made from chip-type feedstocks. For this reason, this perspective paper describes current and potentially viable chip re-use methods from basic principles to final properties. The potential CO_2 savings from chips re-use are also mapped and the ability to process larger scrap is also discussed. The work aims to put into context the value of machining chips which may be otherwise discarded or added to the recycling process chain.

There is currently no literature which summarises the options available for re-use of chips via both solid-state and melt based methods. Wan et al. [13] summarized the representative solid state methods for processing aluminium machining chips, including hot extrusion, equal channel angular pressing, cyclic extrusion compression, friction stir extrusion, high-pressure torsion, screw extrusion, and solid state recycling based on powder metallurgy. However, [13] focuses only on aluminium alloy. This scope should be expanded to consider the potential for re-using steel chips and other materials as well. In addition, there is a particular need to frame the challenge from the perspective of CO_2 emission savings as well as the attributes and downsides of the various re-use options. Existing work in this topic falls short of attempting to quantify the impact of chip re-use on CO_2 emissions. This paper approaches this by dividing uses of machining chips into the solid-state and melting based processes, and offers a perspective on options for chip re-use. In addition, the paper summarises the entire process chain from the mechanism of chip generation to consolidation.

2. Chip formation and separation

2.1. Chip generation and chip size control

Machining is a critical process in production engineering, and includes any process in which a cutting tool is used to remove small chips of material from a workpiece. The three primary machining operations are turning, milling and drilling. By definition, these processes generate chips which can vary significantly in size. It can be generally said that smaller sized machining chips are more versatile and useful feedstocks for a larger range of manufacturing operations, and therefore the generation and control of chips should be well understood. There are several methods of reducing chip sizes for potential re-use. These include the use of: cutting parameters, on-tool chip breakers, vibration, coolants and specialty breaker apparatus [14,15]. These methods can be classified according to three basic mechanisms: self-breaking, breaking upon contact with the tool and breaking upon contact with the workpiece. Chip breakers improve chip breakability by reducing chip curl radius, leading to more effective chip control. A smaller radius leads to more effective chip control and earlier chip breaking. A schematic showing the principle of chip breaking is shown in Figure 1(a-b).

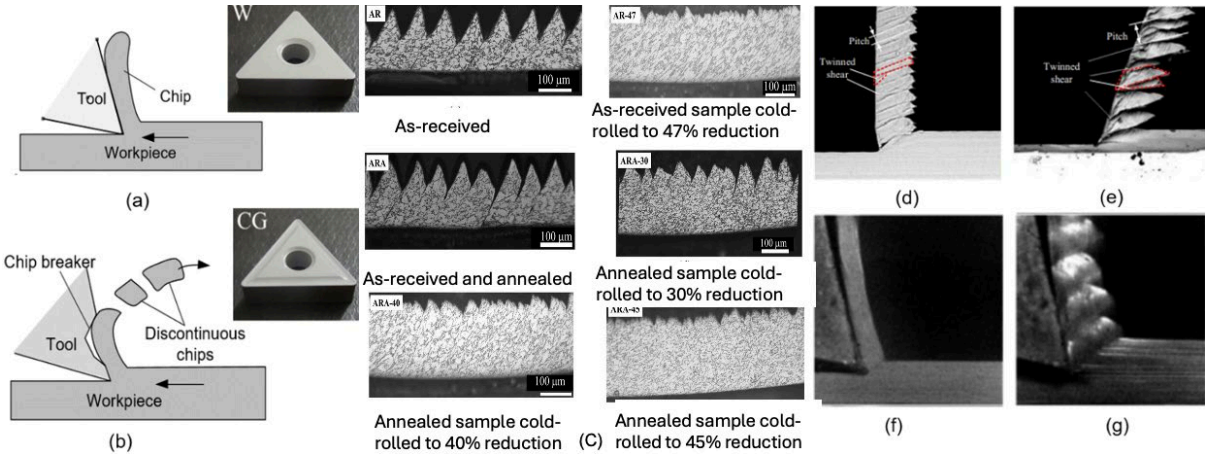


Figure 1 Schematic of (a) normal machining in a typical turning scenario compared to (b) with using a chip breaking principle, with inserts from [16] (c) Chip types in stainless steel produced at varying

turning parameters when using a chip breaker [17], Chip morphology at different rake angles [18]: (d) 5deg, (e) -25deg; and different feed rates [19]: (f) 0.1 mm/rev, and (g) 0.3 mm/rev

The chip breaker can either be an obstruction type device attached to the tool-chip interface, which acts to inhibit chip flow, or it can be a groove type device on the tool surface. In the case of the groove type breakers, the reduced contact area between tool and chip acts to interrupt chip flow, resulting in finer chips [20]. Chip breaker patterns can also be manufactured on diamond cutting inserts using a laser [21]. Chip breaking grooves can also be placed on drilling tools [22]. A demonstration of the effect of a chip breaking dot, laser deposited onto the rake face of the turning tool is shown in Figure 1 (c).

Generating discontinuous chips is favourable for the machining process itself due to several factors. These include friction and therefore heat generation due to curled chips rubbing against the tool, scratching of the workpiece (and tool) by continuous chips, and rapid overfilling of the chip receptacle due to poor compaction of continuous chips. These benefits should be considered on top of their potential use as feedstocks for manufacturing processes, given their better compressibility and flow in the non-continuous form.

Cutting parameters have also a strong influence on chip shape and dimensions [23]. For example, increasing feed rate and decreasing the rake angle can decrease the chip curvature radius and generate severely serrated chips, leading to increased chip fragility [15]. As shown in Figure 1 (c), even when a chip breaker is used, machining parameter selection is still key to successfully reducing chip size. In summary, it has been shown that chip breakers are effective at reducing chip size in many types of steel including 18MND5 low alloy [19], 1045 medium carbon [24] and stainless steel [25]. When considering a re-use process which will use a chip or swarf based feedstock, chip morphology is critical to the feasibility of the process, be it a solid state or melt based technique. This can be also influenced by the workpiece material state, e.g., workpiece texture, strain hardening, as shown in Figure 1 (c) [14]. It is clear that many typical chip types may not be compatible with these processes by default, however several options exist which can be easily implemented to reduce and control chip size without significantly impacting overall performance.

In mechanical machining, lubricants are often used to reduce tool wear and maintain accuracy and speed of the machining operation. Despite this, there have been trends recently to move towards using less cutting fluids in machining operations, as well as dry machining [26]. Many of these present an opportunity as part of the drive towards generating chips capable of being re-used without the presence of contamination. To overcome the rapid deterioration of workpiece surface integrity and tool life associated with dry machining, an ultrasonic elliptical vibration assisted cutting (UEVC) method can be used [27]. A schematic of the principle of this process is shown in Figure 2.

(a)

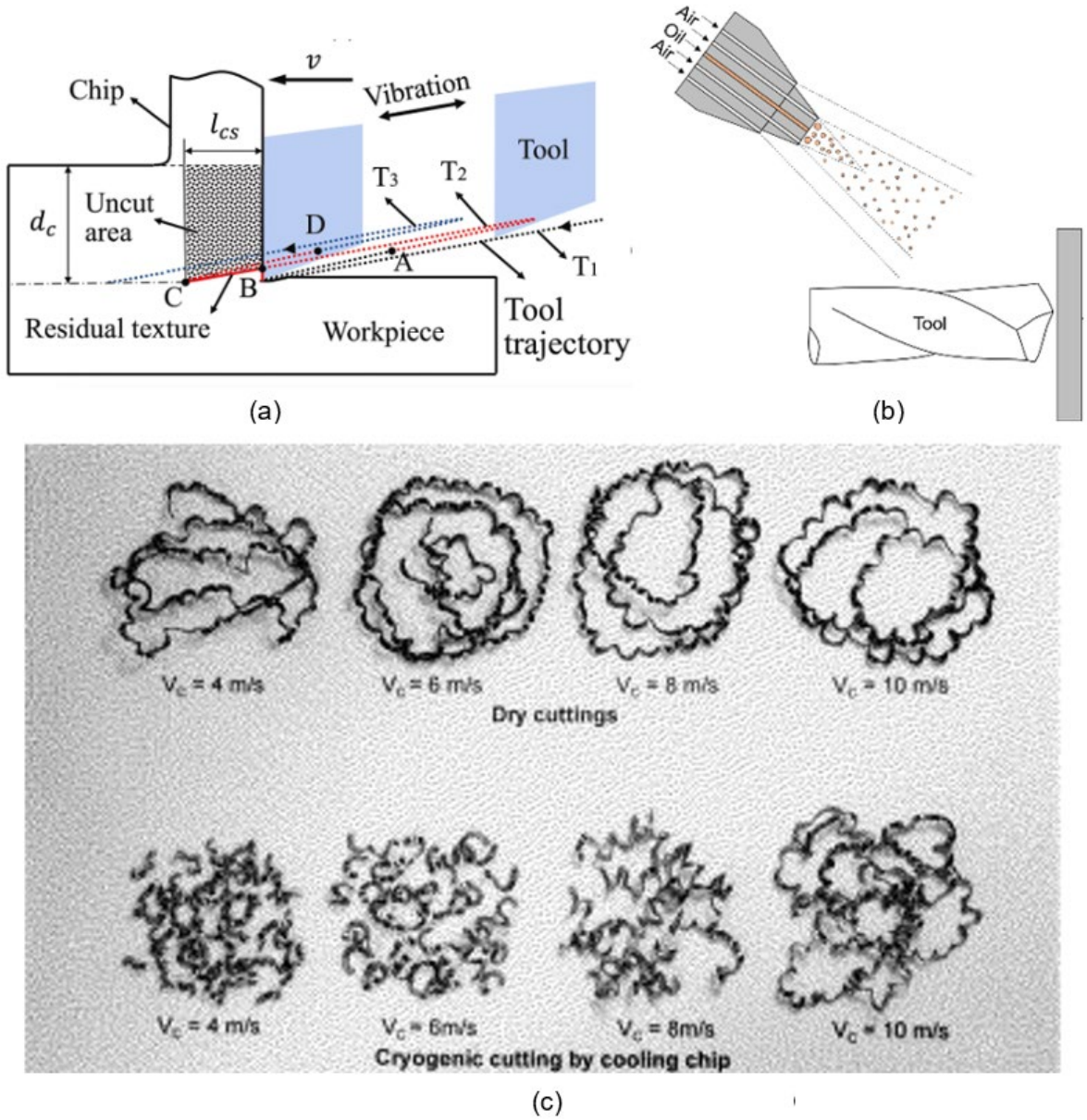


Figure 2 Schematic of (a) machining by ultrasonic ellipitical vibration assisted cutting [28]. (b) aerosol based minimum quality lubricant delivery, adapted from [29]. (c) The effect of cryogenic machining on chip size compared to dry machining [30]

In UEVC, contact time is greatly reduced between tool and workpiece. Due to intermittent contact between tool and workpiece, cutting heat generated is dissipated quickly. For example, when cutting Ti-6Al-4V alloy with a polycrystalline tool, shorter and more regular chips are produced, when using UEVC, along with a reduction in tool wear, in comparison to without the ultrasonic addition [27].

Other concepts useful for minimising the total coolant applied to the machined material include minimum quantity lubrication (MQL) and cryogenic cooling. Minimum quantity lubrication (MQL) is a concept involving a significantly reduced total amount of cooling lubricant supplied to the machining area. In MQL, typically an aerosol system provides a mixture of oil and air. A 2-channel system in which oil and air are supplied separately into a nozzle, producing an aerosol mixture spray towards a tool, is shown in Figure 2 (b). In MQL systems, the overall quantity of oil provided to the machining area is significantly

lower than with conventional cooling lubricants. Workpiece material type plays a key role in deciding whether dry machining or MQL is suitable for the machining operation. In particular, avoidance of adhesive tool wear is critical to the function of the cutting process. Increased temperature as a result of reduced coolant delivery can exacerbate this via material softening phenomenon. Softer materials such as brass, magnesium and cast iron are the most suitable for dry or MQL machining, followed by cast and wrought aluminium, and ferritic steels followed by austenitic steels [29]. The characterization of chip metallographic structure under MQL and dry turning of hardened SAE1045 steel demonstrated that the use of MQL causes more fragile structure of the machined chip than dry condition, which is related with the segmented chip formation. The microstructure of the machined chip under MQL did not change with various tool wear condition, while the tool wear caused modification of chip microstructure under dry cutting, which is due to elevated temperature and stress when tool wear occurs [31]. Cryogenic cooling of the machining chips pre-breaking can be used to lower the temperature of machining chips by localised cooling [30]. Without localised cooling by this method, the cutting resistance of the workpiece would increase. Figure 2 (c) shows example chip sizes produced in steel through localised chip cooling. As well as allowing greater chip breaking during machining, the LN2 based cryogenic coolants are immediately returned to the atmosphere without leaving residue or contamination on the workpiece or chips. In addition, the machining of hardened stainless steel FV520 B under mixed liquid nitrogen-compressed air jet show that the increase of cutting speed and the decrease of jet temperature cause the increase of the serration degree, pitch, and shear angle of machined chips, therefore facilitating the chip breakage [32]. Yıldırım et al. [33] evaluated the chip morphology in machining of NI-based alloy 625 under MQL, cryogenic cooling and combined CryoMQL conditions, with the SEM images of the chip morphologies of front and back sides shown in Figure 3. The results show large scratches due to the severe friction at tool-chip interface in cryogenic cooling, while MQL and CryoMQL cooling significantly reduce the scratches. This indicates better lubrication capability of MQL in reducing the tool-chip friction coefficient. Larger serration occurred in cryogenic condition due to its higher cooling effect compared to MQL.

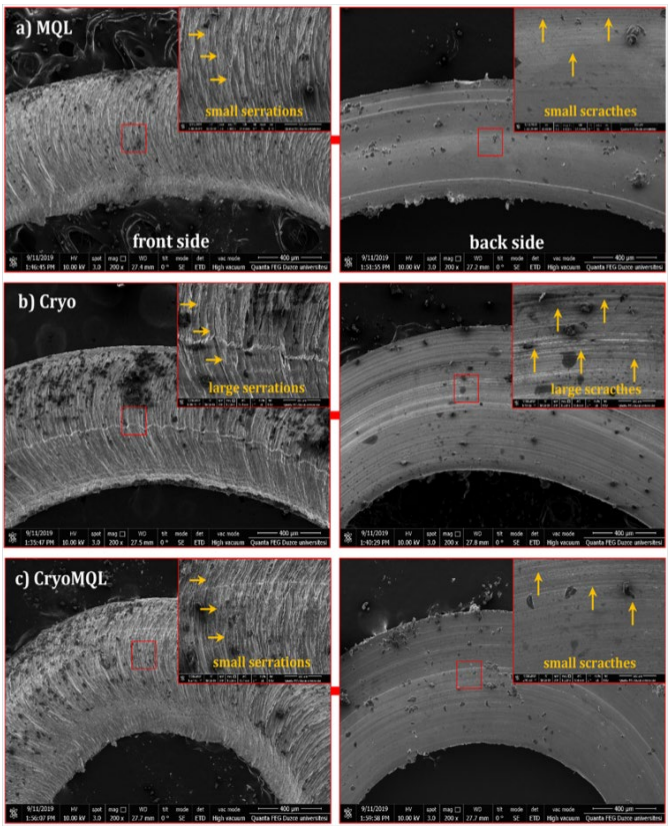


Figure 3 Chip morphologies of front and back side under cutting speed 75 m/min and feed rate 0.1 mm/rev when using (a) MQL, (b) Cryo, and (c) CryoMQL [33]

2.2. Chip microstructure and properties

Microstructure is important to the mechanical performance of metal parts. Specifically, a reduced grain size increases material strength via grain boundary strengthening, down to a grain size of ~10 nm. In some cases, for steels for example in non-load bearing or non-property critical applications, grain size is not a priority, as the strength of the material is sufficient despite altering microstructure. However, enhancing mechanical properties can in principle reduce the mass of material required to yield a certain load bearing capacity, and therefore consideration of microstructure, and retaining this microstructure into final products, in particular those made via solid state methods, should be considered.

It is well understood that plastic deformation alters microstructure. Severe plastic deformation of metals can result in a substantial refinement in grain size to the sub-micron or nanometre range [34], as well as introduction of dislocations. This severe plastic deformation results in arrays of equiaxed grains with grain boundaries with high angles of misorientation. Severe plastic deformation can take place in mechanical machining. Through control of cutting velocity and contact length between tool and material, it is possible to produce a severely deformed and continuous chip even at high cutting velocities in a turning regime [35].

Although in general significant modification of the material microstructure is expected in machining chips, the extent of grain refinement and microstructural change depends strongly on exact location within the chip. Electron backscatter diffraction (EBSD) is a powerful analysis technique for

understanding the level of plastic deformation in machining chips. Yang et al. [36] used EBSD combined with finite element modelling to map the level of strain, misorientation and grain structure with serrated chips in pure iron generated by high speed mechanical machining (Figure 4(a-d)).

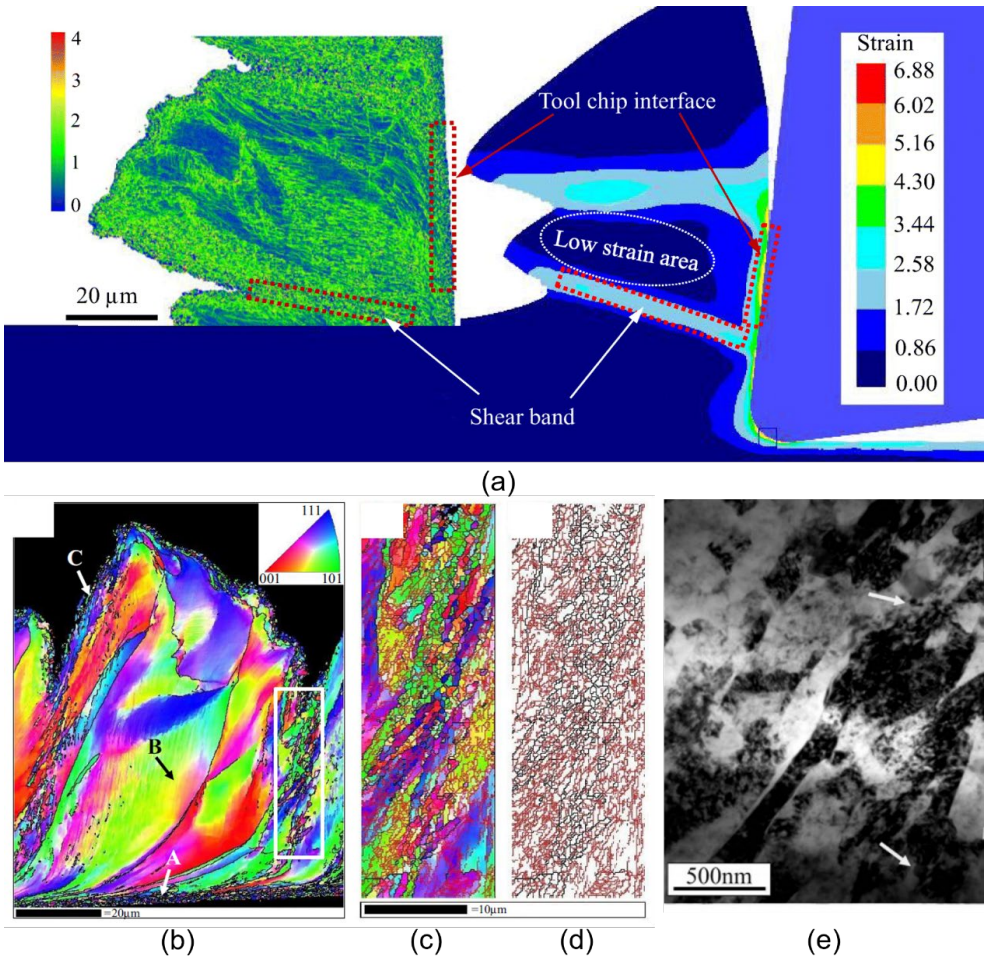


Figure 4 (a) Kernel average misorientation map and corresponding strain levels high speed machined pure iron [36] (b-d) Microstructure of a serrated chip in high speed machined pure iron [36], (b-c) Inverse pole figure maps and (d) grain boundary map of region in (c) with red and black lines representing low-angle (2-15°) and high angle (>15°) grain boundaries respectively, (e) TEM image of sub-micron scale microstructures in chips produced using large strain machining in Al-Mg-Si [35].

In the high strain regions (Figure 4 (a)), significant recrystallization takes place with a large number of grains with high angle grain boundaries (Figure 4 (d)). These regions, for example in the white box in Figure 4 (b), are generally referred to as adiabatic shear band (ASB) regions, whereby the plastic strain causes such rapid chip formation that there is insufficient time for heat to dissipate. In addition a large number of recrystallized grains can be seen at the tool-chip interface (location B in Figure 4 (b)) as well as at the free surface (location C in Figure 4 (b)) – corresponding to the machined surface of the previous cut, explained by friction between the workpiece and tool. A TEM image of a fine grain structure in chips produced using large strain machining of an Al based alloy is shown in Figure 4 (e).

Microstructural characterization of the chip in the machining of normalized AISI1045 conducted by Courbon et al. [37] is shown in Figure 5. Through the observation of the microstructure in the secondary shear zone located at the tool-chip interface using a Field Emission Scanning Electron

Microscope (FESEM), three deformation regimes are identified as shown in Figure 5 (c). These include Region I, consisting of highly equi-axed nanometric grains (≤200 nm) with no preferential flow direction; Region II, composed of equi-axed grains but with a larger diameter (0.3–1 µm); and Region III, characterized by a mix of fine equi-axed and highly elongated grains (≤500 nm). The results confirm that grain refinement takes place under extreme loading conditions during the chip formation process.

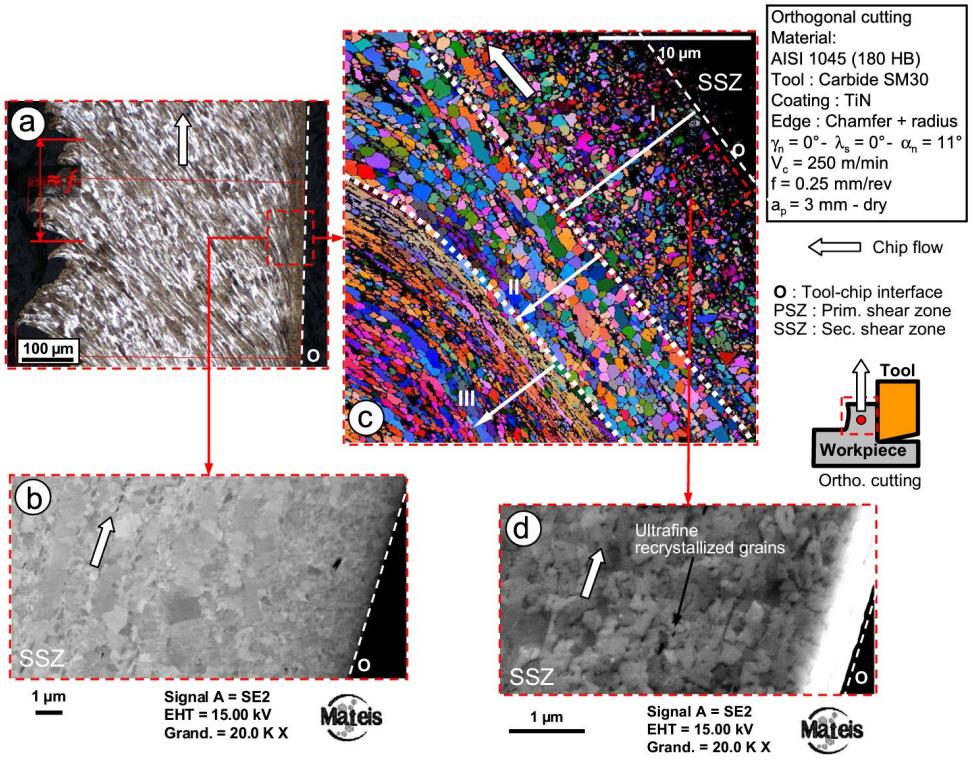


Figure 5. FESEM analysis showing (b, d) a highly recrystallised grain structure in the secondary shear zone and (c) EBSD highlighting the crystallographic orientation [37]

In summary, it can be said that it is well understood that significant recrystallisation and grain refinement is expected to take place in metal chips generated via machining processes, although the extent of such changes will undoubtedly depend on machining conditions. Such microstructures should be considered when choosing a chip type feedstock for re-processing, in particular via solid-state routes.

2.3. Chip cleaning and separation

The impact of coolant reside used in typical machining operations on the final properties of parts made from typical contaminated chips is not currently understood. However it is clear that to for chips to become a viable and reliable feedstock in manufacturing, the composition prior to processing should be known and predictable. In addition, machine tool chip receptacles may mix different material types on a regular basis, and therefore methods for separation in such situations should be considered. This section does not aim to provide in depth guidance for chip cleaning but rather summarise the potential options.

Cutting fluids have four functions [38, 39]: (1) Cooling, (2) Lubrication, (3) Removing chips from machining area and (4) Preventing corrosion. The cooling function is the most important factor, ultimately reducing tool wear. There are four types of cutting fluids. Straight oils, soluble oils, synthetic fluids and semisynthetic fluids. These different types have different attributes which make them attractive in different situations, including ease of maintenance, filterability, lubricity, heat removal and risk of fire. Therefore separation systems should be able to tackle all cutting fluid types. There are several methods allowing separation of contamination and fluid from machining chips. Lee et al. [40] also provide a summary of options for separating chips and cutting fluids. In effect there are three practical separation methods for chips and cutting fluids: magnetic, centrifugal and membrane based.

There are several types of separation system which are appropriate for filtering chips from cutting fluids. Firstly, a magnetic separation system is a relatively simple setup for removing ferrous swarf and chips from used cutting fluid. Ferrous swarf is attracted to the magnetised surface of a rotating drum, after which clean cutting fluid is returned to the cutting machined. A schematic of this is shown in Figure 6 (a).

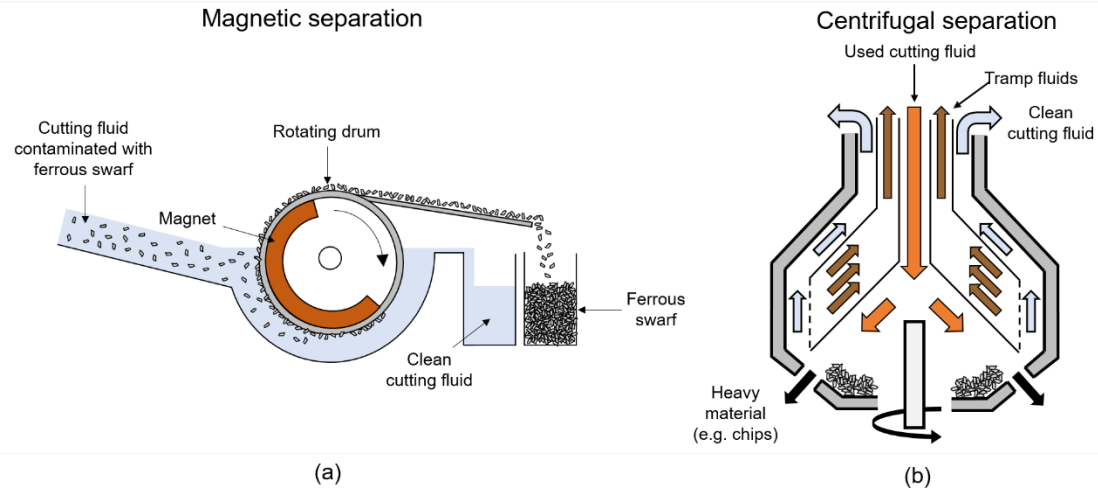


Figure 6 (a) Magnetic drum and (b) centrifugal separation technique for ferrous swarf, adapted from [40]

A more advanced physical separation system is a centrifugal separation setup. The centrifugal force causes heavy material such as chips to be forced to the outside of the bowl. The system also allows the separation of used fluid into clean cutting fluid and tramp fluid. A schematic of this setup is shown in Figure 6 (b). To encourage successful centrifugation, coagulant salts can be added to the mix. It has been shown that up to 96% separation of oil from water is possible using centrifugation [41]. In summary, cleaning and separation systems to separate contaminants and cutting fluid from machining waste are available and can be readily applied, although contamination with other chip material types of similar density and magnetic properties undoubtedly presents a greater challenge for separation and purification. Despite the opportunities for separation and cleaning of machining chip type scrap, the principle and aim of machining chip re-use is to ultimately eliminate process steps between chip generation and feeding into a manufacturing process as a feedstock. In this sense, cleaning steps

represent barriers to adoption of chip re-use in practical industrial scenarios, and should be used only selectively if possible.

3. Chip consolidation and re-use

This section aims to guide the reader through the principles of material densification and consolidation by both solid state and melt based methods. The two approaches are kept distinct for this purpose, as ultimately the method of densification and the barriers preventing their use by both methods are entirely different. To depict the practical advantages of direct chip re-use as opposed to conventional recycling or even a more conventional direct conversion route, the steps in the process chain for all routes are shown in Figure 7, using aluminium recycling as an example in this case.

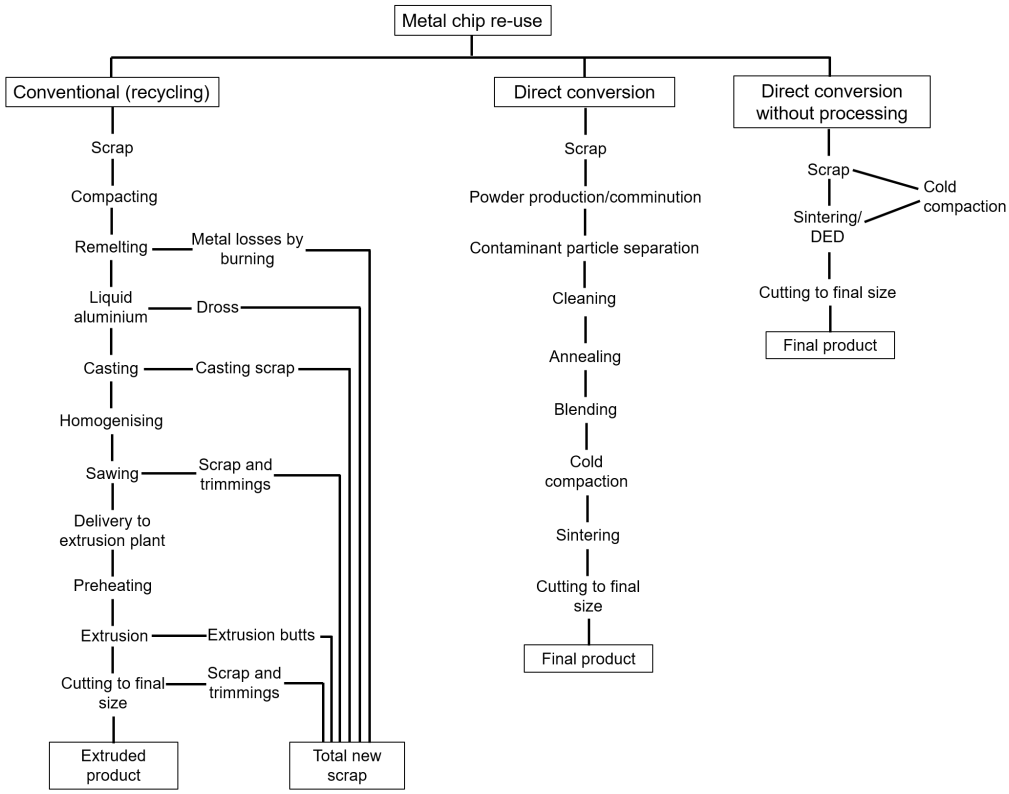


Figure 7 Flow chart of conventional recycling of metal scrap compared to a conventional direct conversion option, and a direct conversion option without processing, adapted from [1]

The flow chart shown in Figure 7 is adapted from Samuel's [1] proposal for direct conversion of aluminium scrap into sintered parts, which is expected to result in a significantly reduced overall scrap rate and has a reduced number of process steps. The direct conversion without processing route proposed here is the ultimate aim of chip re-use, whereby a scrap type is generated ready for direct use in a manufacturing process, effectively replacing versatile feedstocks such as powders. This perspective paper therefore aims to create and present the building blocks to allow the manufacturing community to pursue this objective.

3.1. Solid state consolidation

3.1.1. Densification

The solid-state consolidation methods effectively share the same underlying mechanism of solid-state material joining, and this mechanism will be described in this section. Solid state joining of powder or granular type materials can be described as sintering. This process takes place by diffusion of atoms through the microstructure. A schematic of sintering mechanisms for a system of two particles adapted from Rahaman [42] is shown in Figure 8.

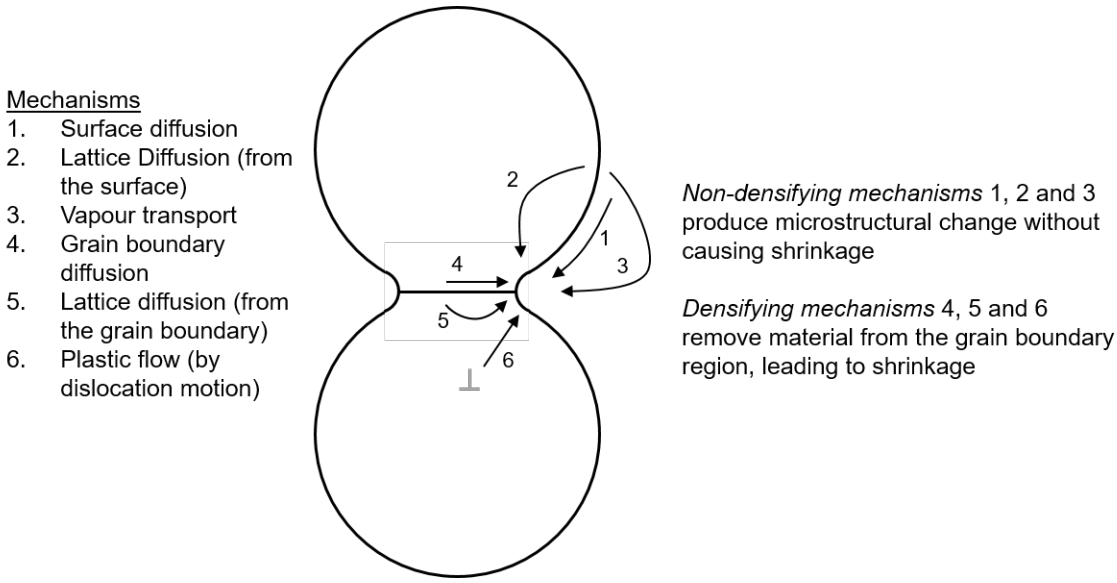


Figure 8 Sintering mechanisms for a system of two particles, recreated from [42].

There are six mechanisms by which sintering of two particles of crystalline material can occur, which are divided into non-densifying and densifying mechanisms [42]. Vapour transport, surface diffusion and lattice diffusion from particle surfaces to the neck of the combined particle, lead to neck growth and coarsening of the particles without densification. The densifying mechanisms of grain boundary diffusion, lattice diffusion from the grain boundary to the neck and plastic flow cause neck growth as well as densification/shrinkage. When the densifying mechanisms dominate, a dense final product is favoured [42]. Grain boundary diffusion and lattice diffusion are the most important densification mechanisms in metals and ceramics, and plastic flow in metals is thought to contribute to the initial stage of sintering, although this depends on initial dislocation density.

When two rough surfaces are joined together, ultimately relying on diffusion bonding to densify, void shrinkage, the first requirement in diffusion bonding, takes place. Void shrinkage is based on several mechanisms: deformation, including plastic and creep, and diffusion mechanisms, including surface diffusion, interface diffusion and volume diffusion [43]. Given the irregular surface on parts, or indeed chips, joined by diffusion bonding, only the long wavelength asperities contact well, and as such the limited areas in contact increase the stress beyond the yield point of the material, causing plastic flow and in turn increasing area in contact until the stress drops below the yield point. Creep deformation is also thought to contribute to void crushing by surrounding material. With reduction in void size, migration of the interface grain boundary can occur due to a decrease in pinning force resulting from the presence of voids. A few unclosed voids are expected to remain in the grain and separated from the interface grain boundary. Void evolution during diffusion bonding is shown in the schematic in Figure 9 (a) from

Zhang et al. [43]. In stage 1, large voids are present after initial joining of two surfaces, in (2), the amount of voids reaches a maximum, in (3), the amount and size of voids decreases and finally in (4) a few voids become trapped in grains after interface grain boundary migration.

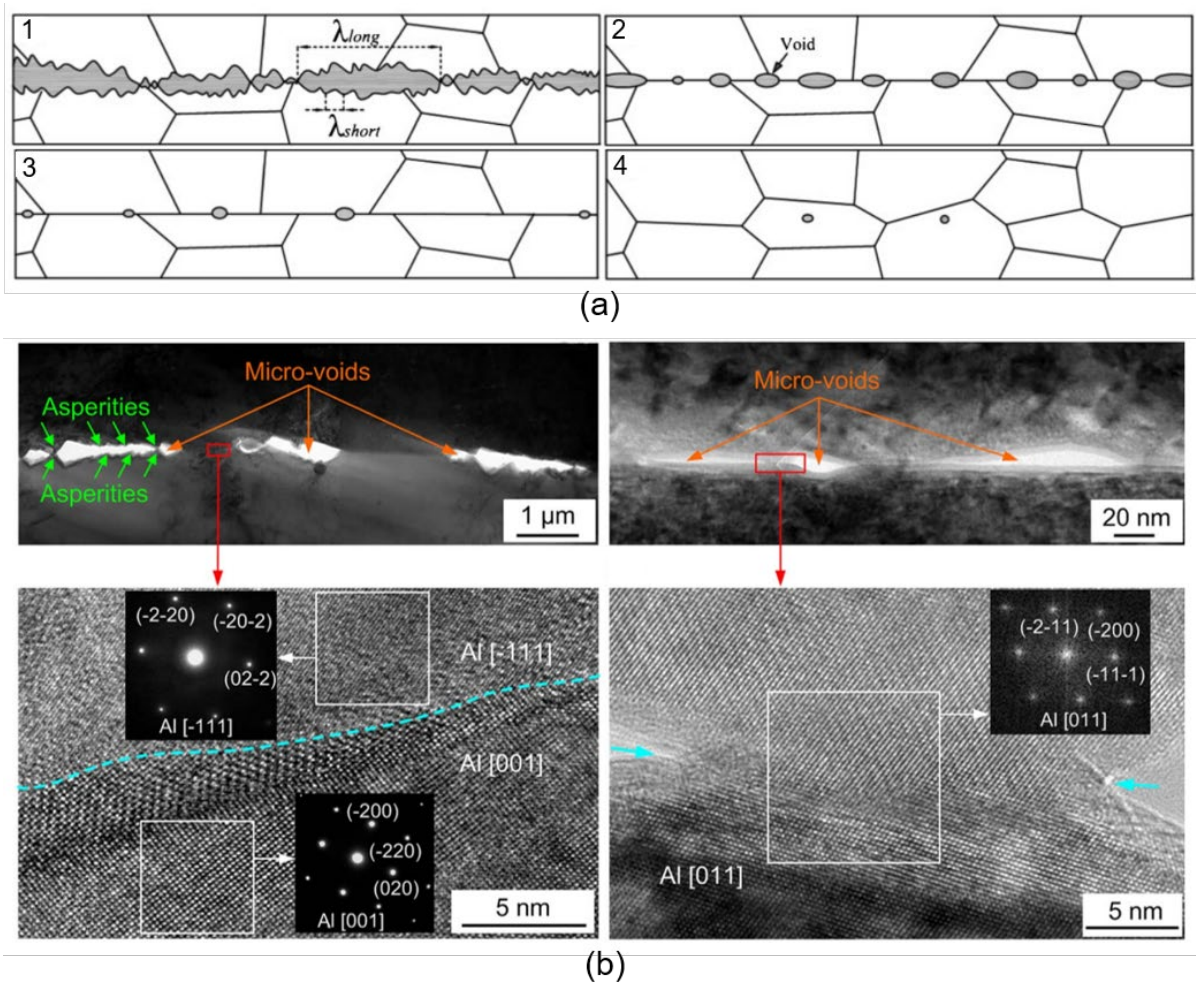


Figure 9 (a) Schematic of evolution of voids by diffusion bonding [43], showing (1) large voids after initial joining of two surfaces, (2) void amount reaching a maximum, (3) amount and size of voids decreasing and (4) few voids becoming trapped in grains after interface grain boundary migration (b) TEM images of bonding interface in weld seams in an Al alloy. [44]

In the absence of a gas pocket, when two grains on either side of the interface come into contact, micro-voids are formed given the micro-asperities on both surfaces. Under pressure and temperature, the metal surrounding the micro-voids plastically deforms, and the surfaces on either side of the micro-voids gradually come into contact to achieve atomic bonding and forming an interfacial grain boundary. This causes the original micro-voids to divide.

In practice, the solid state diffusion bonding mechanism has been investigated and demonstrated, exemplified by porthole die extrusion of aluminium and steel described by Yu & Zhao [44] and Zhang et al. [43] respectively. The quality of the weld seam depends on the presence or absence of a gas pocket. In the case of an aluminium alloy, in the absence of a gas pocket, two different types of bonding interface have been seen [44]. In one case interfacial grain boundaries exist in contact areas, along with micro-voids in non-contact areas. In the other case, in the absence of gas pockets, there are no

interfacial grain boundaries in contact areas and only nanoscale voids exist in non-contact areas. The dimensions and geometry of the extrusion/welding chamber in the die are key factors in determining the presence and absence of a gas pocket. The presence of a gas pocket leads to the formation of a bonding interface with nanoscale voids and amorphous layers, negatively impacting the part properties. Increasing the chamber depth and increasing extrusion speed can reduce volume of micro-voids.

The consolidation of specifically chip type materials by solid state methods is not well understood, but ultimately the underlying principles of particle-particle and surface-surface joining apply and the above mechanisms will define the joining mechanisms. However it is clear that further direct and in-situ observation of chip densification processes should be performed to fully understand chip behaviour.

3.1.2. Inter-particle oxide films

It is well understood that the presence of stable oxide films on the faying (contacting) surfaces of many materials can prevent the achievement of high quality bonds made by diffusion methods. Aluminium based alloys for example have adherent, chemically stable oxides which are insoluble in the aluminium matrix at all temperatures, preventing full metal to metal contact at the joint interface [45]. Given the lower ductility of most oxide films, they can rupture when the parent materials are subject to a large amount of plastic deformation. Alternatively, to exacerbate the oxide rupturing phenomenon, using a rough surface finish on the two faying surfaces can cause greater localised plastic deformation and greater oxide fracturing and in-turn a better metal-to-metal bond. Another route for encouraging disruption of the oxide layer is to use active alloying elements in the alloys, which may chemically interact with and break up the continuous oxide layer, resulting in an array of discrete oxide particles, and better metal-to-metal bonding.

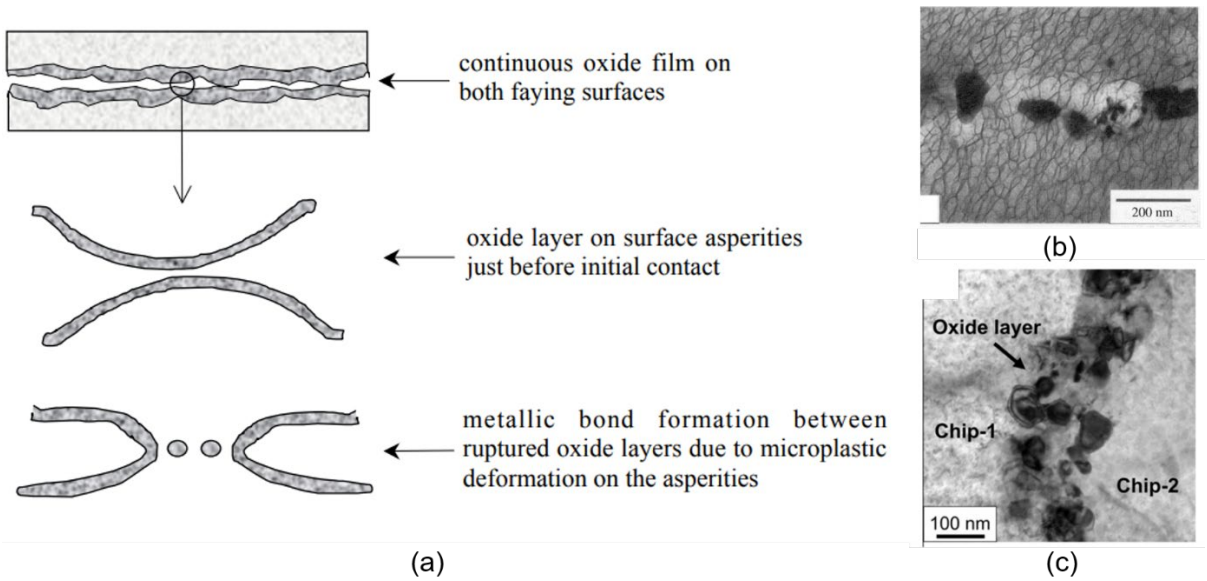


Figure 10 (a) Schematic diagram of solid-state diffusion bonding of materials with stable oxide layers, where metallic bond formation initially occurs between the disrupted oxide layers at contacting surface asperities [45], (b) Transmission electron micrograph of aluminium bond in Al-8090 alloy showing transformation of continuous oxide layer into oxide islands with metallic bonding between the oxide particles [45], (c) a continuous oxide layer between two Ti chips after equal channel angular pressing at 590°C [46]

Figure 10 (a) shows the evolution of continuous oxide films on two faying surfaces to be joined in the solid-state. The oxide layers on the two faying surfaces generally have low ductility in comparison to the metal, and therefore are prone to fracture and rupture. The high roughness level leads to higher stress at multiple asperities and therefore greater rupturing. Metallic bond formation then occurs between ruptured oxide layers due to microplastic deformation at the asperities. However this process inevitably leads to islands of oxide remaining within the structure. An example of oxide islands can be seen in the TEM image in Figure 10 (b), with good metallic bonding between the oxide islands. Of note is the large network of dislocations visible indicative of significant plastic deformation. In Figure 10 (c) a relatively continuous oxide layer between two Ti chips after equal channel angular pressing can be seen via TEM. Although seemingly quite continuous, the oxide regions have still formed islands to some extent. In summary, the presence of oxides on powder or chip surfaces is critical to the bonding and ultimately the integrity of parts produced from these materials. This phenomenon may be a particular concern for material exposed to high temperature and left in air for long periods, such as machining chips, and therefore oxide behaviour and impact on properties should be well understood.

3.2. Solid state methods for chip consolidation

3.2.1. Extrusion

Extrusion is a process in which material is pushed through a die of a desired cross-section, allowing complex profiled shapes to be made. The process can be performed with or without heating the stock material, and this may depend on the material type and intended final part properties. There are two basic types of extrusion, known as direct (or forward) and indirect (or reverse, inverted, backwards) extrusion, depending on the arrangement of the extrusion tools. However the principle of part shaping, and densification of a billet type chip-based feedstock remain the same.

The concept and experimental demonstration of re-use of metal chips by extrusion are not new. Gronostajski et al. in 1996 [47] according to our literature review published the first work on the use of extrusion to recycle machining chips, which in this case were of AlCu4 composition and mechanically alloyed with W. However in this case, granulation of the chips into more regular shapes was performed prior to preliminary pressing then extrusion [47]. Over 98% density was produced with good diffusion bonding. The authors demonstrated similar work in which aluminium chips were segregated by composition, cleaned and crushed into a granulated material, prior to compaction, sintering and extrusion at 500-550°C [48], yielding a product with a density above 97% and a material usage over 95%.

Since extrusion works by the processing of a bulk stock material, for chip processing, pre-compaction is required [48], however critically granulation or modification prior to the pre-compaction stage is not required [49,50]. In one specific example, relatively large Al chips with dimensions 25-80 mm, 1.5-2 mm thickness and 2-3 mm width were successfully extruded after compaction with excellent ultimate density [51], and feedstocks and resultant microstructures of the dense part are shown in Figure 11 (c) and (d), with a chip+pin feedstock mixture also demonstrated. Cold extrusion followed by cold rolling has also been demonstrated as an effective method of chip re-use in the case of aluminium alloy [52]. This

combination of processes was able to produce mechanical properties comparable to the original ingot. Both the extruded and extruded+rolled specimens yielded a higher proof stress and UTS that the original ingot. Extrusion followed by cold-rolling of billet-compacted aluminium swarf has also been investigated in a collaboration with Boeing and Alcoa, with excellent density and properties demonstrated prior to rolling [12]. Industrial level trials were used to produce cans after cold-rolling of the extruded material.

A process chain of directly using the AA6060 chips without melting has been proposed, which involves the hot extrusion of aluminium chips, followed by flattening, rolling and bending or deep drawing. The bent and deep drawn components shown no significant difference compared to those from cast materials in terms of their capabilities for further forming operations without failure [53]. The oxygen contamination level in each step of the AA6060 chips generation and recycling processes, including turning, homogenization, and hot extrusion were quantified. It was shown that the average oxygen concentration increases at each step, with the most significant increase in hot extrusion process. The main source of oxygen contamination does not originate from the Al_2O_3 oxides which are unavoidable, but is caused by the addition in the recycling processes. Therefore, proper design of the recycling process parameters in each step of recycling is necessary to limit the oxygen contamination [54].

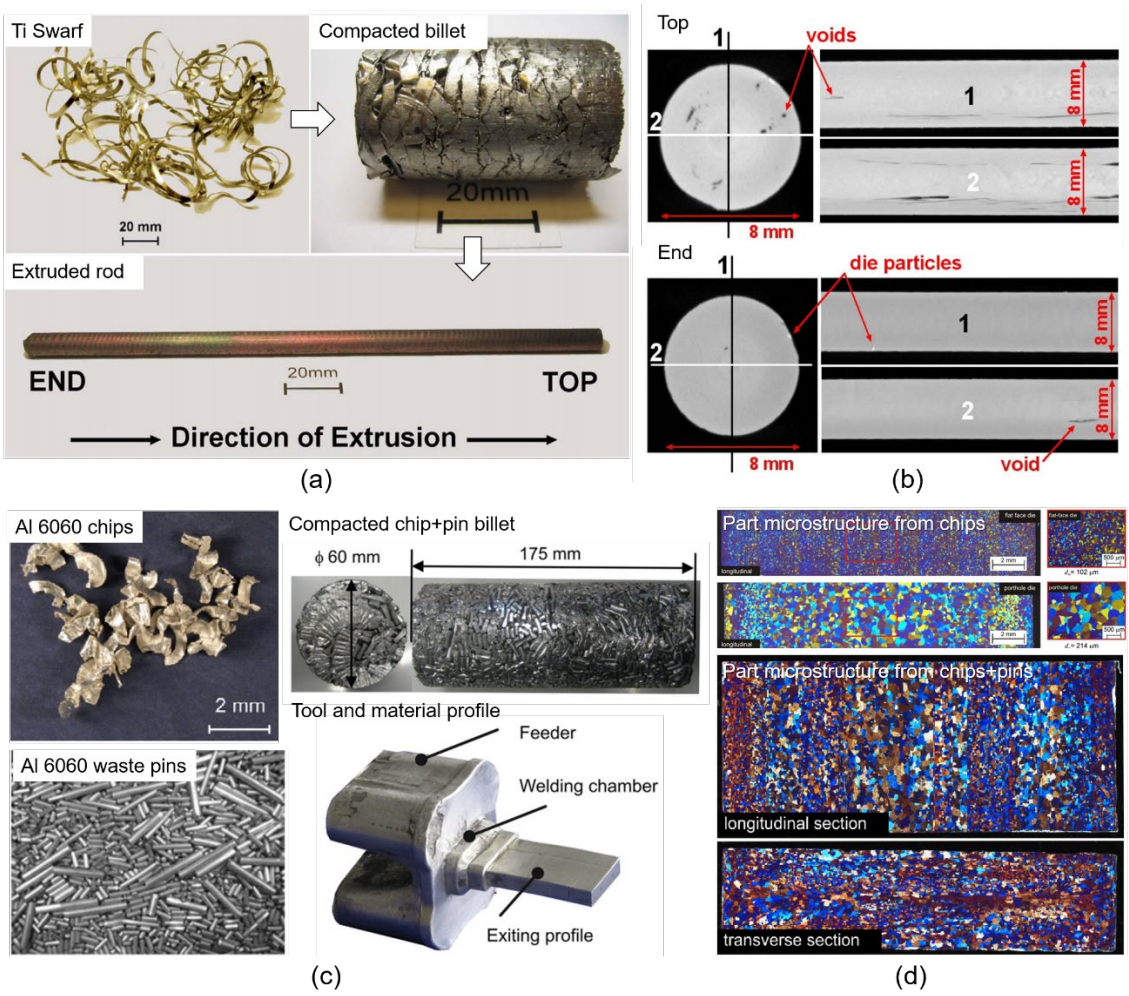


Figure 11 Macro and microstructure of extruded parts from chips (a) [55] Ti Swarf, compacted billet and final extruded rod, and (b) Top and End X-ray computed tomography images showing density/voids according to orientation and position on the rod seen in (a), (c) Hybrid hot extrusion process using a mixture of scrap Al alloy 6060 pins and chips to produce dense extruded parts [51] and [56]. (d) Good microstructure from both chips alone [51] and the chip+pin mixture [56] are seen.

Variations on standard extrusion techniques, which have shown to be successful at chip processing include the KOBO method which involves extrusion synchronised with two directional cyclic rotation of the die [55]. KOBO extrusion involves conventional extrusion combined with cyclically reversible plastic twisting (i.e. a cyclic change in deformation path). This KOBO name is unexplained by the authors/inventors. In general KOBO comprises a group of unconventional methods of metal forming developed to induce significant microstructural refinement and control via external induction of intensively localised plastic flow [57]. In the case of titanium alloy, heating at 350°C was used, below the recrystallisation temperature of titanium [55]. This process can yield contamination free, dense parts with microstructure similar to that of the raw material from which the chips were made [55]. Figure 11 (a) and (b) show titanium swarf, pressed billet and dense rod after KOBO extrusion. X-ray computer tomography images in Figure 11 (b) reveal the high density, albeit with dependence on orientation, of a titanium part produced by KOBO extrusion. Hot extrusion also has been demonstrated as capable of compacting aluminium alloy swarf into a c-shaped channel [52]. Milling swarf and lathe turnings of as-cast Al-Si alloy ingot were cold-compacted into billets prior to extrusion into c-channels at 600 K. Milling

swarf showed superior bonding, density and ultimate tensile strength compared to the lathe turnings. The ultimate tensile strength was still lower than the original ingot however. The extruded material from turnings contained voids, cracks and chip boundaries, indicating a significant difference in compaction behaviour depending on chip morphology and size. The strain ratio of 4.3 for the materials indicated good potential for chips to produce high ductility components. Guley et al. have also successfully produced dense parts via hot extrusion of aluminium alloy, directly from chips [51], as well as from a mixture of waste extrusion pins and machining chips [56]. Scrap prior to processing, the pre-compacted billet as well as extruded profile and microstructure are shown in Figure 11 (c) and (d). The impact of not cleaning machining chips which contain cutting fluid, on performance after hot extrusion [56]. It was shown that the removing cutting lubricant from chips improved tensile strength, however further repeat results are required to draw conclusions with more confidence. Screw extrusion is a continuous solid-state technique for processing aluminium. In this method, aluminium pieces are fed into a chamber where a rotating screw propels the material, heating and consolidating it before it is extruded through a die. Widerøe and Welo [58] conducted the experiments to extrude Φ10 mm aluminium profiles using screws with both single and double flights. Various feed strategies were used to determine the areas of high material flow and dead metal zones in the screw channels and in the extrusion chamber. The experimental results show significant variations of the extrusion speed across different feed rates. Shear Assisted Processing and Extrusion (ShAPE) was employed to process unrefined billets from Al 6063 secondary scrap containing nominal (0.2 wt%) and elevated (0.3 wt%) Fe levels [59]. Due to the severe deformation under high temperatures, the ShAPE process could enhance intermetallic compounds sufficiently to fulfill industry standards for material properties, eliminating the need for pre-extrusion billet homogenization. In addition, a porthole die was incorporated into the ShAPE process to produce various profiles from unhomogenized AA6063 industrial scrap [60]. The results demonstrated a refined and homogeneous microstructure, no detectable weld seams, and the strength exceeding the industrial standards.

The microstructure of parts made via hot extrusion is inevitably modified significantly, and this includes from chip-type feedstocks. It has been shown that grain growth within extrudates in the case of aluminium chips is impinged by the presence of oxide layers at the original chip boundaries. These oxide layers play a key role in material joining - upon breaking down of the oxide layers, metal-to-metal contact takes place and is required for welding of chips and grain growth in these regions [51]. It is also known that die shape can significantly affect grain size [51]. For example Al chips extruded through through a flat-faced die had equiaxed grains with an average diameter of 102 μm, in comparison to 214 μm for those extruded through a porthole die, partly explained by higher temperatures than the maximum profile temperatures in the case of the porthole die in the welding zone [51]. This is explained by additional energy due to higher friction forces. In non chip-based feedstocks, microstructural refinement is expected [61], and strength and ductility have been enhanced via cyclic extrusion compression in Mg based alloys for example [62].

3.2.1.1. Friction extrusion

Another modification of extrusion includes friction extrusion. This process relies on plastic dissipation for heat generation and is a form of severe plastic deformation. Different to conventional extrusion, the extrusion precursor or billet rotates relative to the extrusion die. This generates large sheer stresses and significant deformation particularly in the region in near contact with the die. Heating generated by deformation heating means external heating may sometimes not be required, and the significant level of plastic deformation means solid-state welding of powders (or chips/swarf) is promoted. Friction extrusion is able to extrude densified rods directly from powder without pre-compaction or other processing steps [63]. In addition, significant grain size reduction is often expected due the combined effects of elevated temperature and large deformation. For example, some sub-micron scale grains produced in aluminium powder by friction extrusion are shown in Figure 12 (c) and (d), with before images shown in (a) and (b).

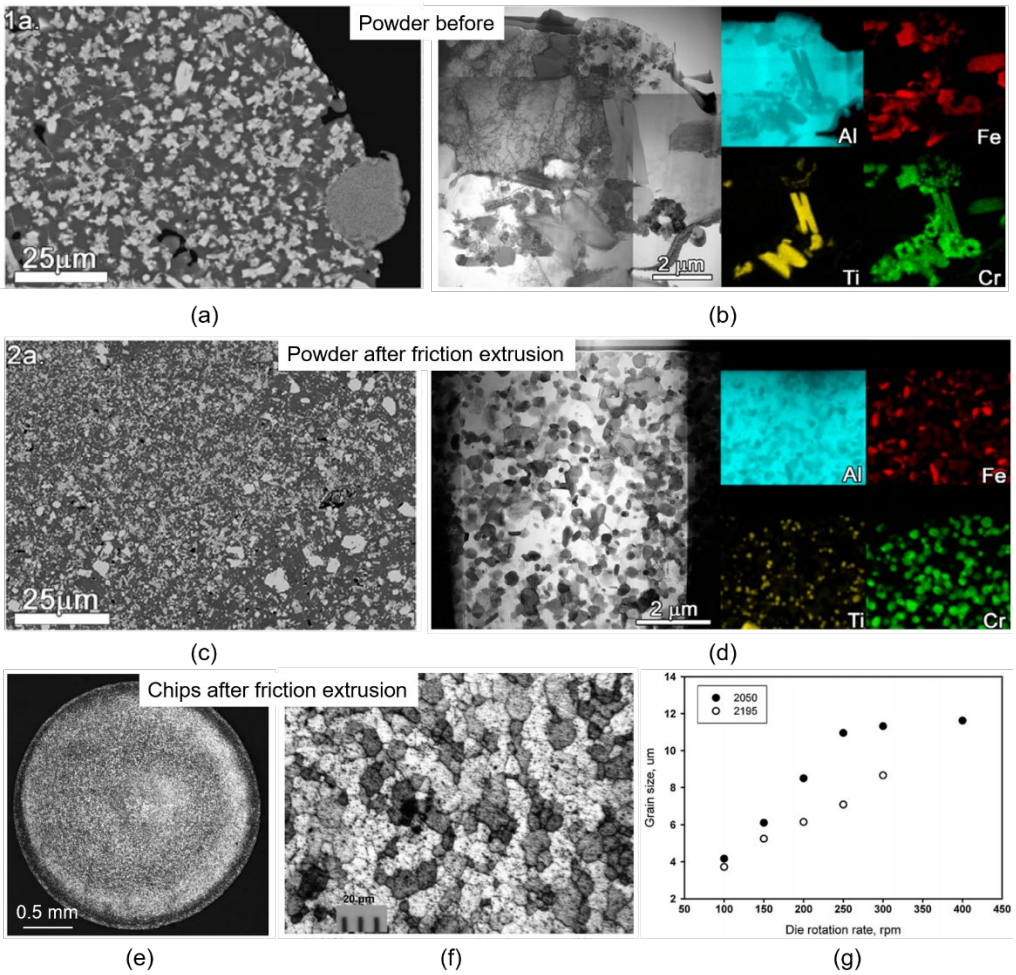


Figure 12 Microstructures of an Al based alloy before (a) and (b) and after (c) and (d) friction extrusion [63], (e) and (f) cross-sectional optical images of structure of Al alloy chips after friction stir extrusion [64], (g) final equiaxed grain size is high controllable with die rotation speed [64].

Friction stir extrusion (FSE) is a feasible process for the compaction and densification of machining chips or swarf into parts. Friction extrusion of aluminium milling chips has been successfully performed [64], with images of the extruded cross-sections at low (e) and high (f) magnification shown in Figure 12. Although pre-compaction was not strictly required, approximately one quarter of the chips were

extruded into a wire, with the rest being compacted into a disk in the billet chamber. Good microstructure through extrusion was produced with high density and an equiaxed grain structure. Average grain sizes increases from ~4 to ~12 μm with increasing die rotation rate Figure 12 (g). Hardness of the wires was generally homogeneous across the cross-sections and properties can be manipulated through process parameters. Good ductility was also demonstrated showing potential for this process route to be versatile. A pre-pressing approach prior to friction extrusion for AA1090 aluminium chips has also been demonstrated [65]. It was shown that defect free wires could be produced, however bulk parts display notable porosity and variation in Vickers hardness. The friction stir consolidation experiments on AA6061 aluminium machining chips reveal two distinct phases: compaction and consolidation in the process. A region with a fully consolidated, bowl-shaped configuration, characterized by recrystallized equiaxed grain structure, is formed at the top of the billets [66]. This process also demonstrates the capability to produce billets with functionally graded properties. By processing chips from two distinct aluminium alloys (AA7075 and AA2011-T3), the graded hardness distributions along the longitudinal axis of the manufactured billet were achieved [67]. A new bonding criterion, named the Plata-Piwnik weighted criterion, was proposed for the friction stir consolidation process of AA7075 aluminium chips. This criterion offers a more accurate prediction of bonding performance compared to conventional criteria with experimental validation [68]. This process has also been demonstrated as successful for processing of magnesium alloy chips [69]. The process has also been attempted as a A continuous process with varying results [70]. Interestingly, the friction extrusion process has been shown to be useful for production of Al-SiC metal matrix composites through processing of aluminium chips with 2 μm SiC powder introduced to the chips before processing [71], indicating the process may be useful for combining multiple materials types of varying hardness, possibly applicable to typical machining tool waste products. The same authors also published work on the energy efficiency of FSE compared to other equivalent chip processing techniques for the processing of aluminium [72], noting that FSE has a better efficiency that ECAP, and both of these are substantially more efficient than the route of remelting the material to produce wire. It should be noted that FSE has been demonstrated so far as successful only for chips of aluminium and magnesium alloy, and steel chips appear not to have yet been processed.

A friction-induced recycling process (FIRP) based on the conform process has been successfully demonstrated for recycling aluminium scraps [73]. The material to be recycled is fed into the groove of a rotating wheel, which is mounted on the output shaft of a powerful geared drive. A tool insert continuously reduces the cross-sectional area of the wheel's groove, steadily compacting and densifying the aluminium chips. Following a quarter turn of the wheel, a counter holder further deflects the material and breaks up the oxide layers. Subsequently, the material is extruded through a shaping die in a manner analogous to extrusion. With the aim of developing a recycling process that optimizes both resource and energy efficiency, it has been demonstrated that the recycled profiles' hardness remains unchanged by the wheel's rotational speed during the stable production stage. Increasing the wheel's speed enhances the throughput when processing low-density particles or chips. In addition, this study suggests that the processing temperature can be elevated by lengthening the tooling system's extrusion channel, attributed to a larger frictional surface area.

3.2.1.2. Extrusion cutting

Forming extrusion cutting (FEC) and ploughing extrusion cutting (PEC) are new methods for effectively combining two processes in one, chip recycling and machining. The processes use a constraining tool to direct cut material and extrude it into a desired shape. In this regard, it offers high efficiency, given direct conversion of chips into grooved strips. FEC and PEC are enhanced versions of an older demonstrated extrusion cutting method for brass [74]. In the case of FEC, in the cutting of pure copper, a forming conservation rate of over 80% was produced, in which high quality grooved strips of higher value were produced as opposed to conventional machining chips. PEC is an improved method from the same research team, which applied two plastic deformation stages during the extrusion process to yield a significant improvement in forming performance [75]. Using this enhanced method, superior grooved strips were produced. Extrusion cutting has been demonstrated only on soft materials of brass and copper, and so requires further evaluation of less deformable materials. The technique is a space and material efficient method of chips of low value from cutting operations and should be subject to further research, although its application to less soft material is not well understood.

3.2.2. Equal channel angular pressing

Equal channel angular pressing (ECAP) is a severe plastic deformation method which was developed to produce ultra-fine grained material. The process is unique as significant cold work is achieved in the processed material without a change in cross-sectional area of the workpiece. To achieve this the material is pressed and extruded around a corner resulting in very high strain. This typically results in rapid deformation of the microstructure due to ultrahigh strain levels (>100%). The microstructure evolution stages are from elongation to coarse to equiaxed to ultrafine with increasing passes in ECAP [76]. ECAP is known to be able to produce significantly higher strength than competing methods in Al [77] for example, in which a yield strength of 630 MPa was produced in 2024 Al. This is explained by hall-petch strengthening and a high level of dislocation accumulation. A magnesium alloy also showed a similar increase in yield and ultimate tensile strength after ECAP to 385 and 455 MPa respectively, owing to an average grain size of 350 nm [78]. Improvements have also been seen in ferritic/martensitic steels [79] by ECAP by producing a grain size of less than 1 μm [80], and producing yield and ultimate tensile strengths of 1.68 and 1.98 GPa respectively [81]. Martensitic lath refinement from a mean between 3.9 and 7.3 μm to between 2.3 and 2.7 μm explained the enhanced properties. Higher strengths in steel are possible by cold drawing of thin wires [82,83], although this has very limited scalability and practicality in particular for processing of chips. Figure 13 shows (a) shows EBSD maps of a steel subject to ECAP at different conditions, revealing the substantially refined grain structure [79]. Luo et al successfully densified and controllably refined the microstructure of titanium chips via ECAP [46], with the TEM image in Figure 13 revealing a chip interior after 8 ECAP passes at 590°C, showing a generally equiaxed structure with some sub-grain boundaries and dislocations visible. Once again, in ECAP, the rupturing of oxides on chip surfaces is critical to metal-metal welding and a good part density and bonding [84]. In addition, as a result of only partial breaking of the oxide layer, it is thought that that chip boundary staying somewhat intact leads to impingement of grain growth (shown in Figure 13 (c)), which may be a benefit in some cases.

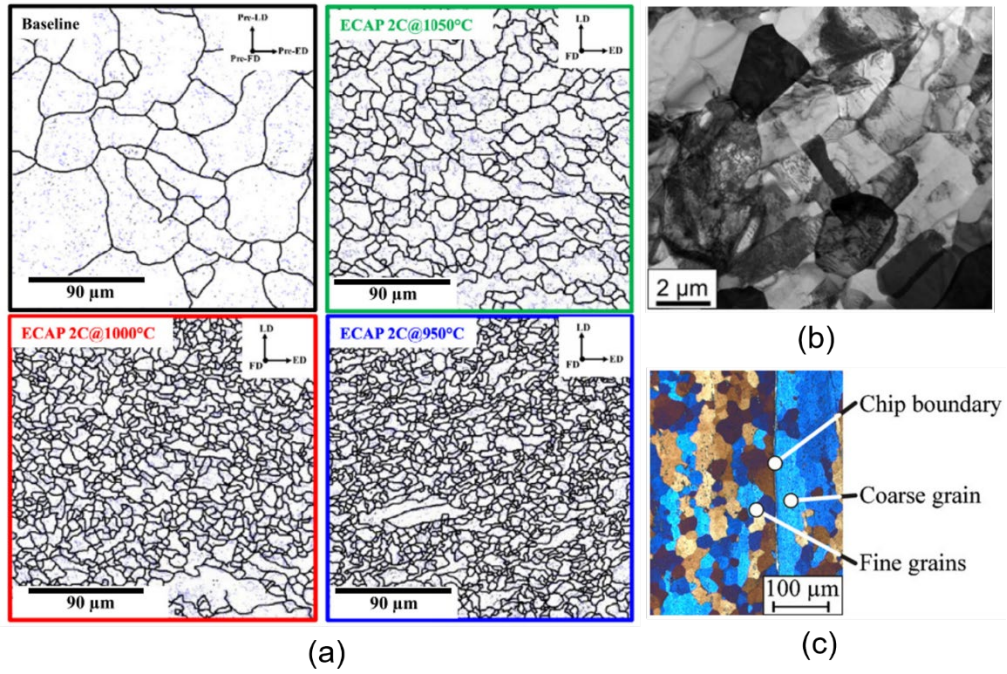


Figure 13 (a) EBSD maps of steel subject to ECAP at different conditions, revealing the substantially refined grain structure [79] (b) TEM image of chip interior after 8 ECAP passes at 590°C, showing a generally equiaxed structure with some sub-grain boundaries and dislocations visible [46] (c) Impingement of grain growth in ECAP by the chip boundary [84]

Equal channel angular pressing (ECAP) has also been successfully used to consolidate titanium machining chips into fully dense parts at temperatures of 450-590°C [85, 86]. The density of parts made from Ti-6Al-4V chips using various numbers of passes and increasing back-pressures has also been evaluated [86]. It was shown that 99.9% density could be reached after 8 passes at 100 MPa, or 4 passes at 150 MPa. The effect of 4 passes over just 1 was significant in terms of density. Ti-6Al-4V machining chips have also been consolidated successfully via ECAP, with the original chip microstructure was refined and rearranged according to the ECAP inclination direction [86,87]. Temperatures between 400-500°C resulting in ~99.9% density products [87]. Hardness could be increased via multiple passes up to an average of 415 vickers hardness, notably higher than the nominal ~350 vickers hardness of the raw material. This can be explained by grain refinement caused by multiple passes through the ECAP system. Using one pass only however, 359 vickers hardness value could be reached using ECAP. Figure 14 shows the general microstructure of ECAP Ti-6Al-4V chips after pressing at increasing numbers of passes.

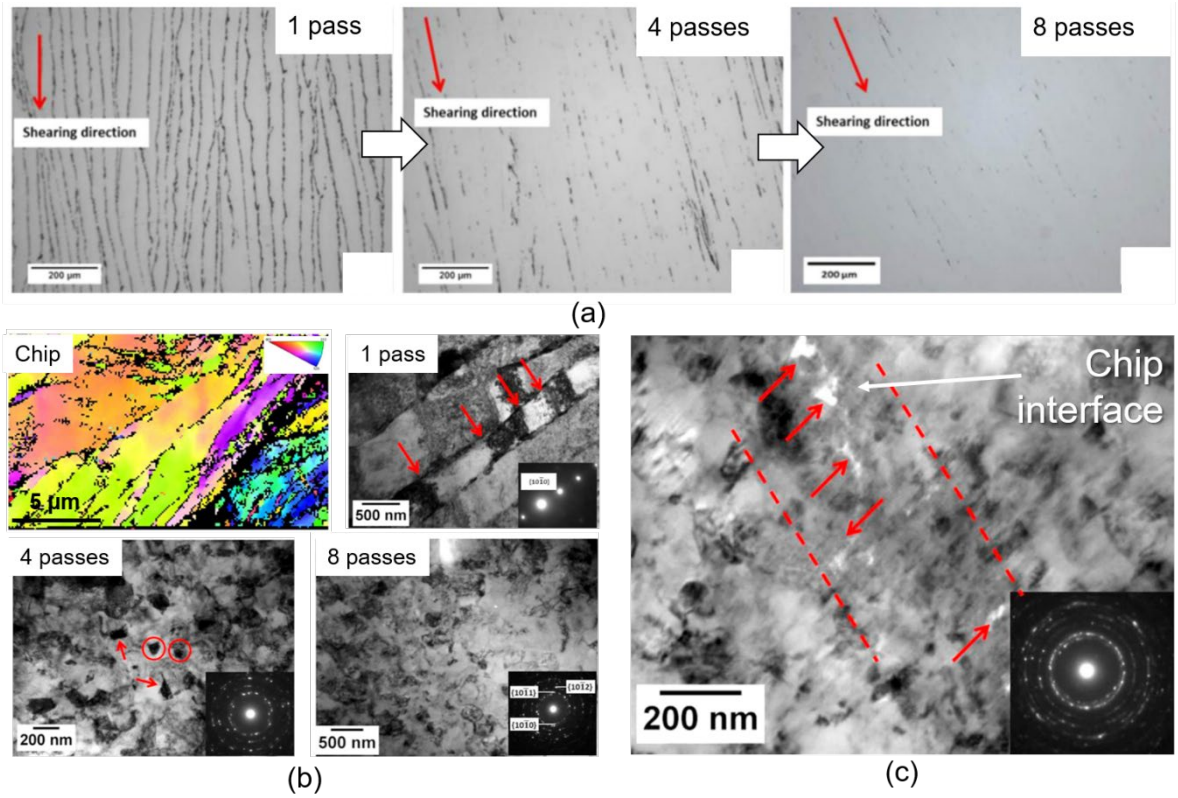


Figure 14 Microstructure evolution in Ti-6Al-4V chips subject to ECAP at increasing numbers of passes by Shi et al. [87] (a) Cross-sectional structure of ECAP part made from recycled Ti-6Al-4V chips at 500°C, with 100 MPa of back pressure, after 1, 4 and 8 passes, (b) Inverse pole figure map of microstructure of raw chips and TEM micrographs of ECAP part after 1, 4 and 8 passes and (c) TEM micrograph of remaining interface between chips in ECAP part subject to 4 passes.

TEM analysis also revealed a fine elongated microstructure at the sub-micron scale after the first pass, which is reduced in size into an equiaxed structure with grains of 300-500 nm after 8 passes. This behaviour is consistent with the expected grain refinement model in this process [88]. Pure Ti has also been successfully pressed using ECAP at 450°C, yielding a similar yield strength to raw ingot of the same composition [89]. Lui et al. showed that final microstructure of Ti-6Al-4V parts made by ECAP do depend on the starting chip morphologies and dimensions, however these differences could be removed through an annealing process, leading to a near-identical microstructure for all parts, consisting of a generally equiaxed α + β structure along with some lamellar α. In summary, ECAP is a promising technique for densification and grain refinement of chip type materials, and a large range of material types including steels may be possible, given as a powder it has been successfully densified and grain refined.

3.2.3. Forging

Hot forging is another severe plastic deformation process which has been demonstrated as a viable method of densifying chip type feedstocks. In hot forging, a malleable metal part is worked into a pre-determined shape by one or more proceses include hammering, upsetting or pressing, before which

the billet is heated to its plastic deformation temperature [90]. Given this process is typically applied to bulk parts, pre-compaction of chips is required prior to forging.

Khamis et al. successfully compacted three chip sizes from AA6061-T6 aluminium alloy produced by high speed mechanical milling, via hot forging [91]. Chip size was not measured but chip size was on the scale of 1-4 mm on the longest lengths. Basic cleaning was performed using an ultrasonic bath with a solution of acetone. Pre-heating of the chips was performed at 480°C to soften the material prior to forging. Forging times varied between 60 and 120 minutes. It was found that chip size, despite not varying significantly, had little effect on the final ultimate tensile strength. It should be noted that cross-sectioning to reveal density was not performed. Although this was a basic study, it was still a proof of concept that hot forging can produced a part with reasonable strength, and therefore the technique should be considered as a viable option for further research. Shahrom produced a densified material also from 6061 chips, using a version of hot forging utilising cyclic extrusion compression back pressure [92]. Here, pre-heating at 550°C was also performed for 2 hours prior to a 60 ton forging press. Smaller chips were correlated with a denser final part with smaller boundaries between chip structures, with boundaries being between 1.2 and 0.5 µm for the smallest chip size, and chip boundaries between 3 and 7.5 µm for the largest chip size (see Figure 15 (a-b).

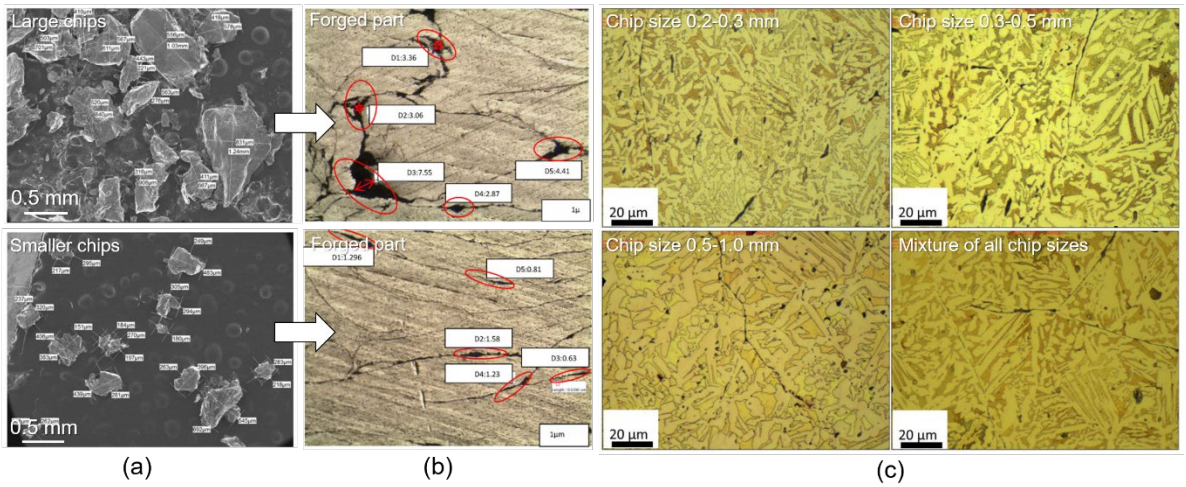


Figure 15 Effect of chip size on density for (a-b) a forged part from aluminium 6061 machining chips [92] and (c) Brass chips of various sizes pressed into parts by hot forging [93]

Hot forging of brass has also been performed after green compaction, and various chip sizes were also investigated as to their impact on microstructure [93]. Pre-compaction was performed at 800 MPa, followed by 750°C forging. Images of the microstructure of these parts is shown in Figure 15 (c). Once again all parts showed some evidence of chip boundaries, and EDX showed only partial diffusion had taken place. Based on the initial studies so far, which are not entirely comprehensive, it is well understood that simple compaction and general densification of aluminium alloys is possible via hot forging, although elimination of chip boundaries has proved difficult. However in cases where 100% density is not critical to the final part properties, hot forging may offer a reasonable option.

3.2.4. Spark plasma sintering

Spark plasma sintering (SPS), also known as field assisted sintering, is a low voltage, direct current pulsed current activated, pressure-assisted sintering and synthesis process [94]. As well as synthesis new compounds, it can be used to densify materials in one step. SPS is similar in terms of processing to hot pressing, however the method of transfer of heat to the sintering materials is different. When the material to be sintered is electrically conductive, heat is dissipated directly from within the sample and from the pressing tool. However when a non-conductive material is used, heat produced by joule heating is transmitted by conduction from the electrically conductive tool. This heat is supplied simultaneously with pressure. SPS is useful for the rapid sintering and densification of materials generally considered hard to sinter such ceramics or nanomaterials [95], and therefore has great potential for chip densification using a range of material types.

Of particular relevance to the processing of chips as well as powders in general, is the ability of the electric field in SPS to contribute to oxide film fracture, and therefore good chip consolidation [96]. The SPS process combined mechanical, thermal and electrical effects [96]. The impact of sparks helps activate the metal surface eliminating surface impurities and enhancing diffusion [94]. Joule heating promotes plastic deformation and material transfer due to very high heating rates and efficient volumetric heating, assisting consolidation and bonding mechanisms via viscous flow and diffusion during sintering [94]. Yield strength is also reduced under applied electric field. SPS pulsed power provides a dispersed discharge point and rapid cooling of the intergranular bonding, and this mechanism stops contributing once necks and bonds are formed between chips [94]. Direct TEM observation of the ability of FAST/SPS to produce a good metallurgical grain-to-grain bond was shown by Groza & Zavaliangos [97]. The experimental result demonstrate clean particle surfaces at an atomic scale, with direct grain-to-grain contact in FAST sintered specimens as shown in Figure 16 (a).

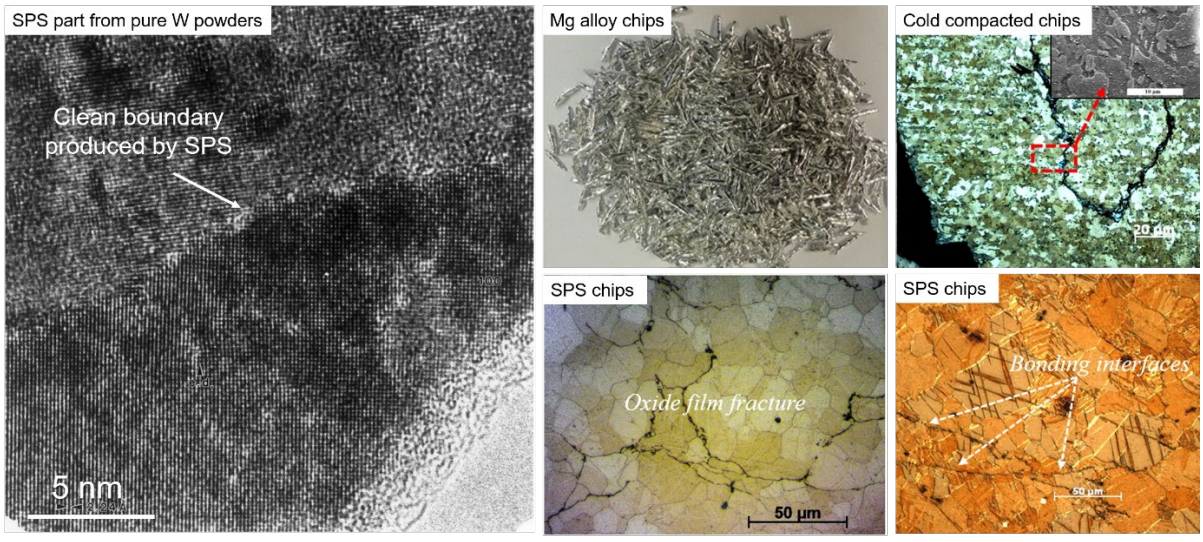


Figure 16 (a) A clean boundary produced from pure W powders by SPS [97], (b) Mg alloy chips subject to cold-compaction and then SPS, yielding excellent bonding with evidence of oxide film fracture, and extensive deformation twinning [96].

SPS has not been extensively researched for its ability to process chips, however magnesium alloy chips were able to be fully densified using SPS at 500°C resulting in sufficient plastic deformation to produce a dense part [96]. Sparse voids were seen in the sintered part, with a maximum size of ~260 μm. Ultimate tensile strength was also improved by between 8 and 19% owing to the decreased grain size as a result of both the initial machining operation, and the SPS process. The authors also demonstrated that SPS could be used to densify a blend of aluminium powder and machining chips at 490°C, with the powder acting as a binder for the chips [98]. The initial particle size of materials in SPS plays a critical role in their densification, however this depends on the melting point of the material. Therefore, for swarf and machining chips, pre-compaction is necessary for effective sintering. In summary, the additional thermal and electrical mechanisms activated by the electrical field in SPS offer some advantages over other techniques, and it is expected that researchers will exploit the process to interrogate chip densification and properties in more detail.

3.2.5. Additive friction stir deposition

Additive friction stir deposition (AFSD), patented by MELD™, is a new solid-state manufacturing technique that combines the working principles of friction stir welding and additive manufacturing (AM). AFSD does not involve material melting, thereby avoiding process-induced defects common in fusion-based AM methods. In AFSD, friction stir heating and an externally applied force collaborate to cause plastic deformation of the metal rod, which is then deposited layer-by-layer to construct a three-dimensional object. The process has the benefits of a high production rate, the generation of an equiaxed grain microstructure, and compatibility with a wide range of raw materials [99]. AFSD demonstrates its effectiveness by utilizing Al5083 waste chips as feedstock, resulting in the deposition of defect-free material that exhibits a refined, wrought-like microstructure with improved mechanical properties [100]. It was shown that although there was a decrease in yield strength, the ultimate tensile strength of the deposited material exceeded that of its wrought counterpart.

Ti-6Al-4V alloy chips were successfully utilized in the AFSD process, with the process schematics, deposited part and its microstructure property shown in Figure 17 [101]. An analysis of the microstructural and mechanical characteristics of the deposited material demonstrate how various deposition parameters influence the quality of the deposited part. It was shown that the deposited material featured lamellar α/β colonies within fine equiaxed prior β grains, with the α phase present at the grain boundaries. The tensile properties of the deposited part are higher than those achieved through other additive manufacturing techniques.

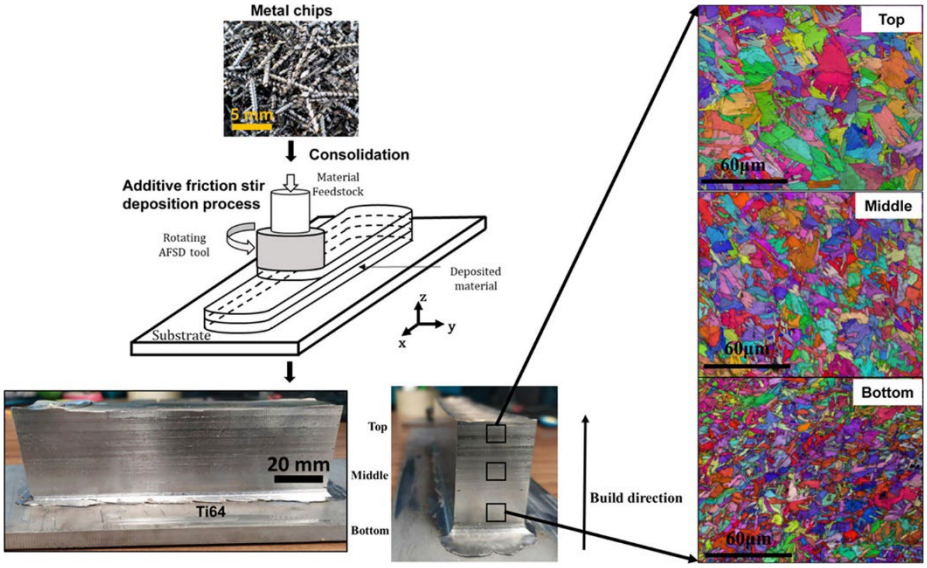


Figure 17 Schematic of AFSD process of Ti-6Al-4V using recycled chips, the deposited sample and its microstructure property [101].

3.3. Melt-based particle incorporation

According to the literature, so far laser based directed energy deposition (DED) is the only method to have been investigated for its ability to process chip type feedstocks. In addition, the process remains a versatile technique for additive manufacturing using a range of feedstock types, including powders and wires of different sizes, of metals and to some extent ceramics. Therefore this section will focus on the principles of melt-based incorporation and densification of powder type materials via DED.

Material deposition by powder blown DED occurs via powder catchment. During typical distances in powder blown DED, it is expected that the particles have insufficient time to interact with the laser beam before arriving at the melt pool [102], therefore they are expected to be solid when reaching the substrate or melt pool, resulting in ricocheting upon reaching the former. The powder catchment zones have been clearly and concisely described by Prasad et al. [102] and can effectively be described as three main regions, illustrated in Figure 18.

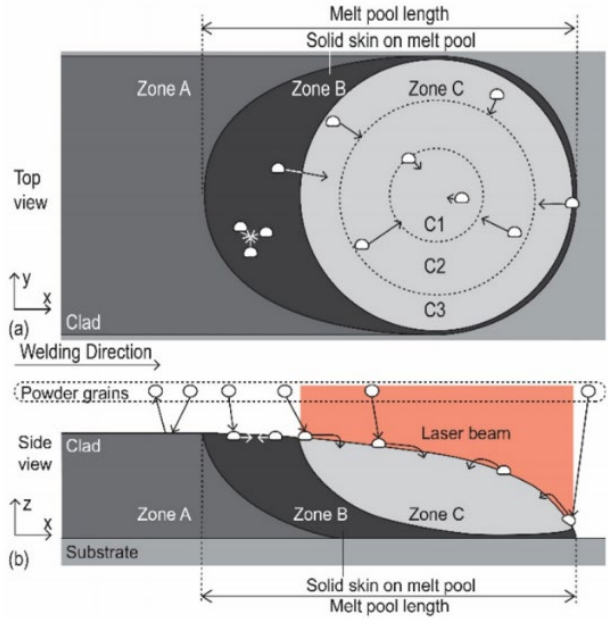


Figure 18 Schematics of powder catchment during co-axial fed powder blown DED [102].

Zone A is solidified regions around the process zone, which include the substrate and the clad. Powders which arrives in zone A ricochet. Zone B is a region of the melt pool outside of the laser spot, and is covered by an oxide layer of a solid skin. Powder arriving here attach to the clad, by forming aggregates or they be fully incorporated if they overcome surface tension before solidification, or if they move into Zone C. Zone C is the region of melt pool irradiated by the laser beam, and powders arriving from all directions are incorporated and move radially toward the centre of the laser spot for a short period before melting. Zone C contains sub-zones of C3, C2 and C1, and are dominated by Marangoni flow. These are the edge, the intermediate region and the centre of the laser spots respectively. The incorporation time decreases nearest the centre of the laser spot. The gaussian nature of the laser beam means material temperature is highest in the centre, meaning powders melt faster in comparison to the edges of the spot, and thereby faster incorporation. Centering the powder stream to the centre of the beam will increase catchment efficiency as well as accuracy of parts. Powders in the intermediate region travel the furthest, followed by the centre then the edge. Powders in the centre (C1) zone need the longest time to incorporate. Powder caught in Zone B, outside of the laser spot takes on average ten times longer to incorporate than powder inside the laser spot.

Prasad et al. [103] used high speed imaging to identify that a “powder island” can form in the centre of the melt pool when a focused co-axial powder stream is used, and this can play a key role in deposition. In this case the laser power is insufficient to melt all arriving powder and powders may in fact ricochet of this region in the centre of the melt pool. The authors summarised their work by identifying three main mechanisms for incorporation of powder grains with the melt, enabling good catchment. Firstly, powders arriving in direct contact with the melt pool are engulfed and melted within a few microseconds. Powder arriving in contact with floating oxides on the melt pool surface take longer to incorporate or may be carrier to the back edge of the melt pool, possibly remaining as surface roughness on the solidified track. Secondly, incorporation can take place through the powder island. A small proportion

of powders arriving at the island ricochet, and the remainder join the island likely aided by powders on the island being molten. The powder island and gradually and constantly incorporated into the melt, and is replenished to a constant size through powder flow. Finally, incorporation can take place via molten droplets or a mushy zone. Powders on the solid skin or the melt pool edges may melt and aggregate to form a molten droplet, and powders arriving contacting this droplet incorporate quickly. These droplets then can incorporate with the melt pool. If this droplet is over-saturated with powders, this may turn into a so-called “mushy zone” and becomes a part of the powder island again.

The mechanisms of incorporation of chip type feedstocks into the DED melt pool have not been investigated as yet. However it is clear that with blown-powder delivery, a critical threshold will exist for the dimensions of a chip which can be incorporated and fully melted by the melt pool. In addition, it is expected that use of an increasingly large chip feedstock will reduce the likelihood of a single particle attaching to the melt pool without rebounding. The present authors are currently interested in the mechanisms of incorporation of chips and this is expected to be a growing area. It can also be noted that wire-fed delivery, with its greater control, may offer opportunities for manufacture of parts from compacted swarf strips, although this has not yet been investigated. Nevertheless, some preliminary work has been performed on the ability of directed energy deposition (DED), also known as laser cladding, to manufacture parts using machining chips from a few material types, albeit with varying levels of pre-processing. However the current state of research in melt-based re-use of machining chips is much less extensive than for solid state methods.

3.4. Melt-based incorporation and deposition of machining chips

When moving to chips from powders, the incorporation of larger chips is undoubtedly more difficult and will yield less consistent tracks and ultimately less accurate parts. The size of chips which can be processed, based on the incorporation mechanisms above, is limited by the dimension of the melt pool (zone b + c). In addition, creation of an island of chips in the melt pool which gradually incorporates is more difficult, given their larger size and difficulty in creating a narrow stream of chips.

Research carried out on chip deposition via DED is not extensive and can be split into work performed using unaltered chips and chips which have been post-processed to reduce their size. Mahmood et al investigated the deposition via DED of chips sieved into different particle sizes [104]. Successful tracks were produced with all chip sizes, with minimal or negligible porosity, although this was not measured in detail. Melt pool widths between 2500 and 3250 μm were generated. Interestingly mean track height reduced and mean track width increased with increasing chip size (see). The authors theorised the melt pool becomes larger when larger chips are used, through reduced beam shadowing effects, however this requires further clarification. The reduced height with larger particles is explained by the reduced incorporation into the melt pool. Interestingly, a reduction in hardness was seen with larger chip sizes, from just over 400 HV to just under 200 HV from the 124 to 418 μm mean chip size. This was explained by larger grain sizes via slower cooling, caused by larger melt pools. The explanation of large melt pools causing slower cooling rates is consistent with prior research [105], although the link between larger chips and larger melt pools needs further investigation. Different chip sizes were produced by varying

the depth of cut. It was found that chip sizes of up to 418 μm diameter could be successfully deposited into walls with no significant porosity, defects or contamination. Images of chips and an example built wall are shown in Figure 19 (c,d).

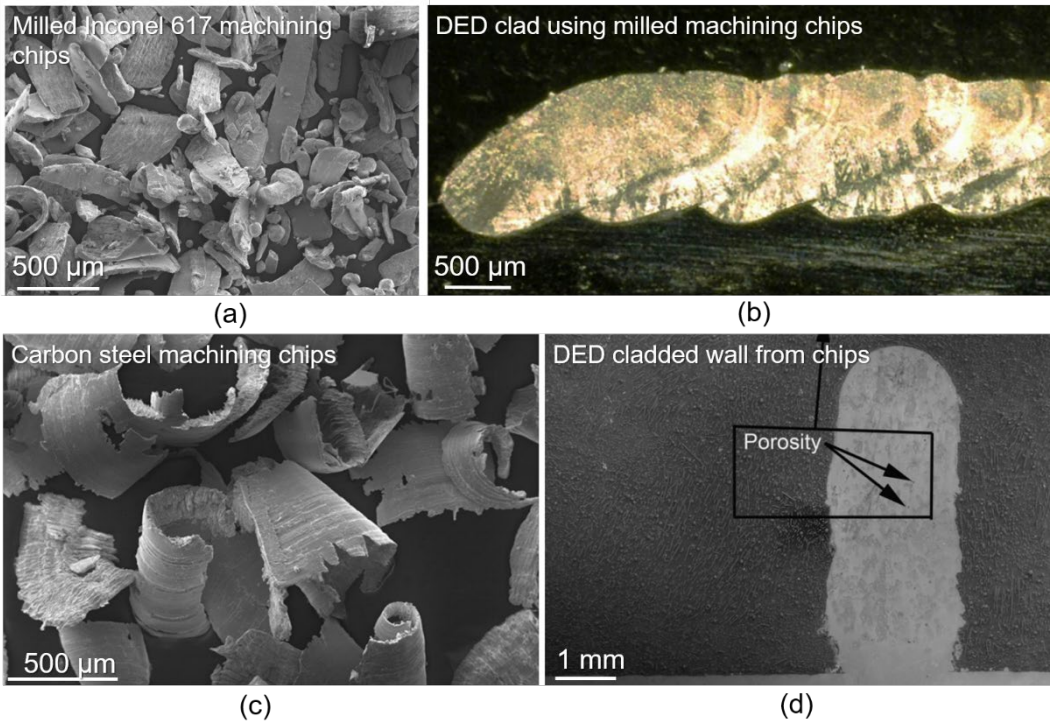


Figure 19 (a-b) DED clad produced from Inconel 617 machining chips after milling to reduce size and ultrasonication [106] (c-d) A DED built “wall” from carbon steel machining chips produced by dry machining [104]

The remaining studies which use a chip based feedstock use post-processing methods to reduce the chip size prior to laser deposition, and therefore do not fully represent the successful incorporation of “chips” directly from a machining operation. Mahmood et al. deposited Inconel 617 milling chips after significant post-processing [106] (Figure 19 (a) and (b)). A significant post-processing operation was used to reduce the 1 mm average chip size to under 300 μm spherical average spherical diameter via ball-milling then sieving with a -50 mesh (also generating waste). Example chips and clads are shown in Figure 19 (a,b). Cutting fluid was used in machining which was then cleaned via sonication, followed by drying. The 1 mm mean chip size was reduced through processing in a disk mill, with the resulting chips passed through a -50 mesh sieve, producing a final powder size with a mean diameter less than 300 μm. Successful cladded tracks were produced, comparable to those produced from a gas-atomised powder. However, in this case, since the chip morphology was altered to a more spherical shape, the study effectively eliminates the factor of the machining operation from the process, and further work should more carefully consider the impact of these post-processes. Jackson et al. [107] also deposited 316L stainless steel chips by DED, however they were again processed via milling, reducing their size to between 45-150 μm, also reducing their angularity. Razumov et al. [108] used a similar processing route of using a grinding bowl and sieving to reduce chip size, prior to successful DED and selective laser melting. Similar work has been performed in which Ti-6Al-4V machining chips were ball-milled for

3 hours, producing a particle size below 50 µm [109]. The material was successfully, densely deposited, with good hardness and fine microstructure. Mahmood et al. also produced machining chips by milling a medium carbon steel bar under dry conditions [104]. Interestingly it was observed that an increase in feedstock chip size was correlated with a decrease in hardness. It was theorised that the larger chip sizes increased melt pool size, effectively reducing cooling rates, thereby increasing grain size. However further analysis is needed to explain this correlation. Nevertheless this study showed DED may be appropriate for direct deposition of dry cut machining chips.

Noticing the absence of work on the impact of unprocessed chip conditions on the ability of machining chips to be processed by DED, the present authors recently carried out a study on the impact of coolant on chip processing by DED [110]. As part of this work, no processing was applied to the stainless steel chips prior to deposition via DED through pre-placement and vibrational delivery.

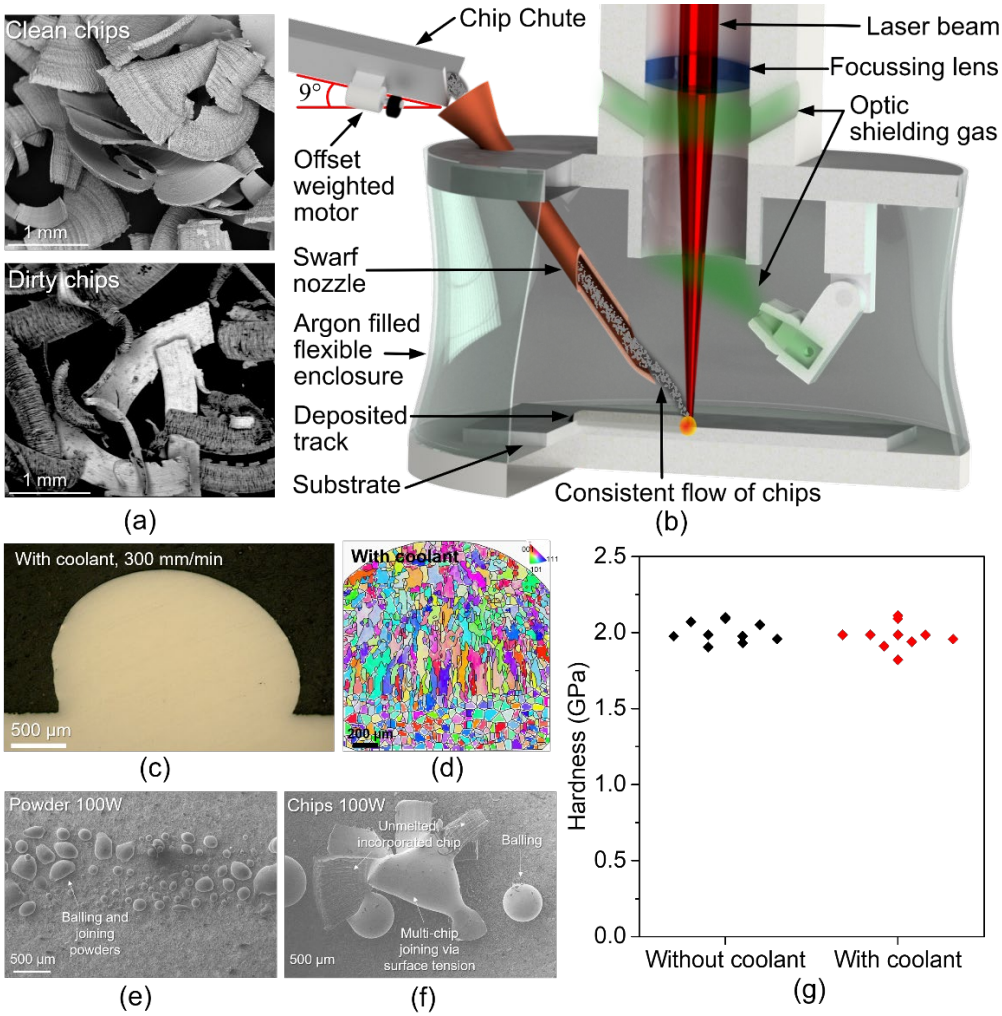


Figure 20 Work by the authors demonstrating directly fed chip deposition via DED [110]. The study clarified that coolant is eliminated by laser interaction and does not influence final chip hardness.

In this work, it was observed that coolant residue present on chips (visible in Figure 20 (a)) created by milling played no role in the final properties of the DED tracks. The hardness (Figure 20 (g)) and elemental composition was the same for both “clean” and “dirty” chip feedstocks. In addition

microstructure appeared unchanged and no visible porosity was introduced by the presence of coolant (Figure 20 (c) and (d). Low power laser scanning was used to interrogate the balling and melting mechanisms of the chips compared to the powder (see Figure 20 (e) and (f)). Despite the much larger size of the chips, the relatively thin dimension correlating to cutting depth, of 100 μm, is thought to have aided the rapid balling of the chips and attachment to the workpiece. Therefore, chip thickness likely plays a key role in ability to readily melt. A bespoke feeding system (Figure 20 (b) was developed to feed the unprocessed chip feedstock as a powder, and repeatable, consistent tracks were produced, demonstrating the potential of chips to be a versatile feedstock. Further work in this area should cover the question of maximum chip size which can be incorporated and how it relates to laser focal distance and melt pool size.

Although only basic work has been performed so far on laser based deposition of machining chips, it is clear that chip size plays a role in the ability to be deposited as a dense track, as well as the properties of that track. This is despite DED being relatively insensitive to powder/chip size, in comparison to selective laser melting for example, which shows much higher sensitivity to powder size. For this reason, convenient methods of reducing chip size should be considered for its potential application.

Fullenwider et al. [111] used a dual-stage ball-milling strategy to reduce the size of 304L machining chips into powder with a desirable morphology with 38-150 μm particle size. Nanoindentation also showed the ball-milled powders exhibited a higher hardness than the equivalent gas atomised powder based on nanoindentation testing. An example of stainless steel chips produced at University of Nottingham by dry milling, and the same chips after simple ball milling are shown in Figure 21.

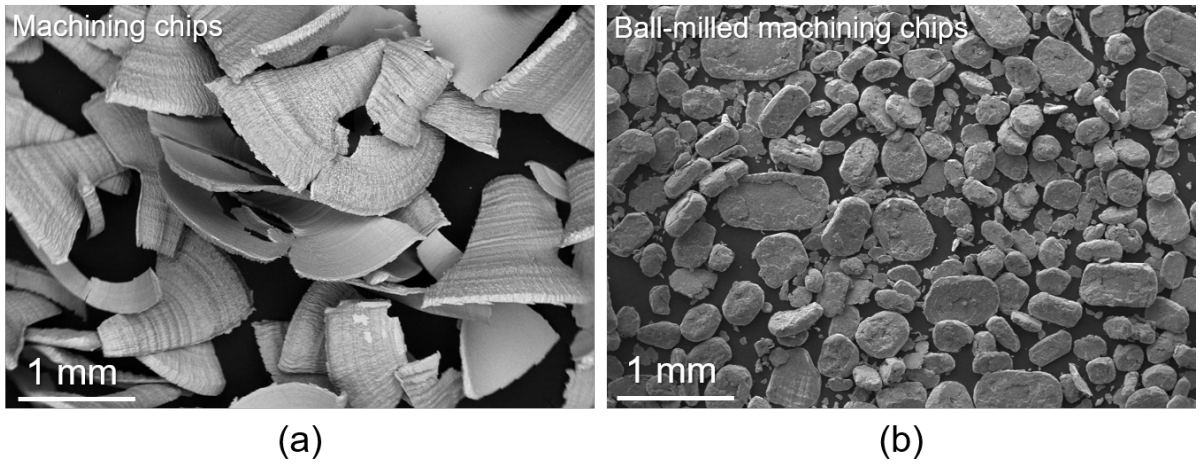


Figure 21 Clean machining chips from stainless steel produced by dry milling (a) before and (b) after ball-milling

A clear reduction in chip size can be seen in Figure 21 after 1 hour of ball-milling. The surface morphology is generally improved as well, which is a critical factor for delivery of such materials, in particular for melt-based processed such as DED. It is clear that ball-milling can be used to manipulate chip size for re-use, however the energy requirements and practicalities around adding this process step should be carefully considered.

4. The case for re-use of machining waste – an emissions perspective

This work so far has presented the opportunities for chip processing from the perspective of the quality and density of product which can be produced. This metric is undoubtedly critical to the practical adoption of chips as a feedstock in any capacity, and will determine the economic drivers for their adoption. However, recent environmental and political drivers for reduced CO_2 emissions, means consideration of new methods to mitigate emissions, including via material re-use, may become mandatory.

To understand the potential CO_2 emission savings from re-use of machining chips, it is important to breakdown the end-use of steel, given its much larger contribution to global CO_2 emissions than any other material type. We can use the case of the UK to consider the breakdown of steel end-use according to waste vs yield. Figure 22 shows the breakdown of manufacturing end-use using steel in the UK, ordered according to absolute % resulting as waste.

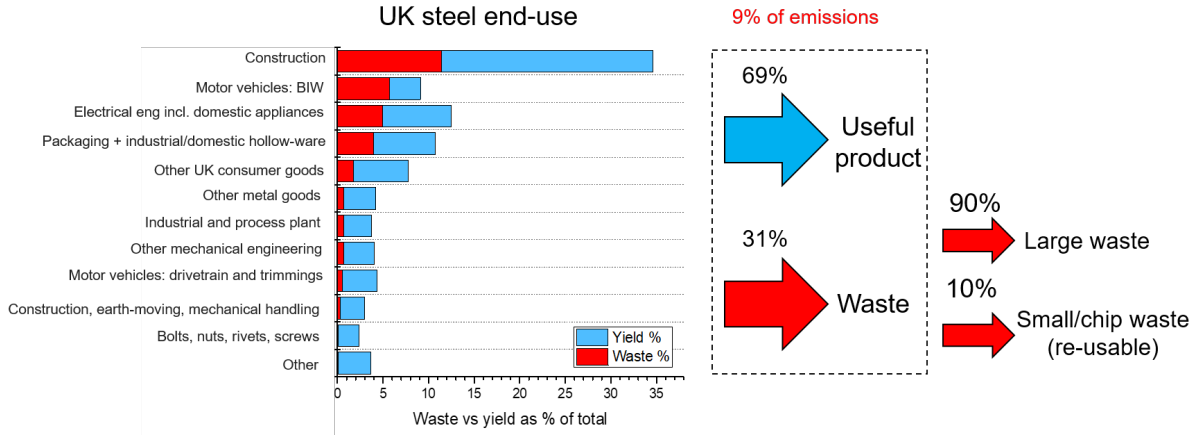


Figure 22 Breakdown of steel yield vs waste % based on end use, and proposed form of this waste. Construction has not been included. Data is from the International Steel Statistics Bureau [112].

In the breakdown in Figure 22, some assumptions are made regarding the form of the waste produced according to end-use. For example, waste from body-in-white motor vehicles is expected to be of the form of cold/hot stamping and forming offcuts, and can be classified as "large" as opposed to a potentially re-usable chip feedstock. Chip-type scrap can be classified as more "re-usable" as they are more easily fed or placed into current manufacturing processes which normally require a powder, or relatively fine feedstock. This assumption was made also for steel attributed to electrical engineering, appliances, packaging and hollow-ware. The other sub-categories are expected to contribute a much larger proportion of waste of smaller turnings, chips and swarf. A conservative assumption on this leads to a prediction of 3% of all UK steel being in the form of machining waste, i.e. chips/swarf.

The potential emissions savings generated from re-use of this waste into useful products, which would otherwise have been made from non-re-used material, must be considered from the perspective of much of this scrap currently being recycled. If we make the assumption that 100% of machining chips and swarf are currently recycled, emissions savings can only be made by avoiding the emissions associated with recycling. It should be noted the environment impact is different among various

recycling technologies. For example, a life cycle assessment of aluminium alloys chips recycling through single and multi-step friction stir consolidation process [113] shows that the single-step process offers a significant reduction in environmental impact compared to the traditional recycling pathway. However, its environmental benefits are affected by the inefficiencies of the non-productive transition phase and the variability of the energy mix used in producing electrical energy. In contrast, multi-step processes yield billets of higher hardness and more uniform grain size distribution. Thus, from a multi-objective standpoint, the higher environmental cost of multi-step methods may be compensated by the improved quality of the recycled components. An environmental assessment [114] of solid state recycling routes for aluminium alloys shows an overall impact reduction by a factor of 2 for the SPS route and 3-4 for the extrusion routes when compared with the corresponding remelting route as the reference. For steel, primary steel production has a fivefold higher CO_2 emission intensity compared to secondary/recycling production based on UK data [115]. Taking the approximation of 10% of all UK scrap steel ending up as chips, applying this to global emissions, re-using all chips is expected to save **0.1%** of global CO_2 emissions through avoidance of recycling. This 10% "re-usable" manufacturing scrap, is also supported by prior work [12]. If we assume 0% are currently recycled, 100% re-use of machining chips is expected to yield a **0.5%** saving of global CO_2 emissions, based on the fivefold higher CO_2 intensity of emissions from primary steel production. Although difficult to obtain the rates of recycling based on breakdown into small and large scrap, the fraction of annual discarded material that becomes part of future production is thought to be 65% for steel [116]. Hence, based on this ratio, the potential CO_2 savings from re-use of chips is **0.24%** of global CO_2 emissions, i.e. 65% closer to the 0.1% value than the 0.5% value. However it is likely that the machining waste recycling rate is much lower than the 65% figure, and hence potential CO_2 savings are likely to be higher. In the above calculations of CO_2 emissions, the effects of logistics are not specifically analyzed. However, it should be noted that the chip re-use process benefits from co-locating the facilities for manufacturing and re-use. As a result, the logistics costs associated with this re-use strategy are naturally lower compared to those of the conventional recycling process. It should be noted that with expanding the category of machining chips into offcuts from stamping, forming and casting, the potential re-use category expands to up to 20% of all steel, and therefore potential savings can increase by a factor of 4 to a maximum of 1% of global CO_2 emissions which is the estimated contribution from melting of all scrap. Hence there is an argument for steering such processes to yield smaller scrap and offcut geometries.

To summarise the calculations above, Sankey diagrams for the flow of steel in manufacturing, with global CO_2 emissions, are shown in Figure 23 (a-c). It should be noted that in these calculations, we make the assumption that re-use of material replaces like-for-like processes which are already currently used.

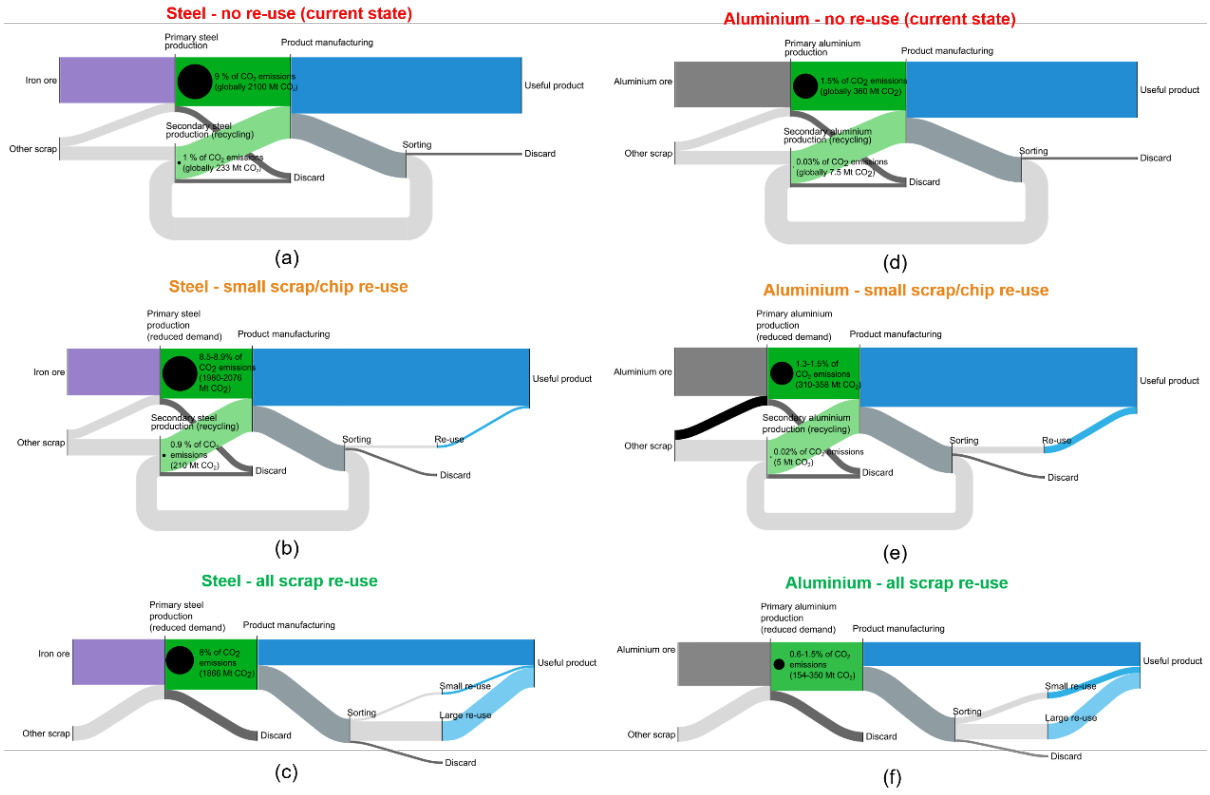


Figure 23 Sankey diagrams illustrating (a-c) steel and (d-f) aluminium flow in manufacturing and associated global emissions, before and after re-using all small scrap/chips and after re-use of all scrap.

According to the 'Net Zero Roadmap 'report published by the International Energy Agency, the global crude steel production in 2022 was 17.4 times that of aluminium production. Additionally, the direct CO_2 emissions from iron and steel were 9.6 times those of aluminium [117]. However, given aluminium is not generally produced for construction, a larger proportion of aluminium is produced for smaller manufactured components. Global data is difficult to obtain, however, as an example, it has been claimed that 25% of German manufacturing aluminium scrap is in the form of chips [118,119]. If we assume the 25% value is representative of global data, and assume a total scrap rate for aluminium similar to that of steel, i.e. 31%, based on the 25% scrap:chip ratio, 7.8% of all aluminium ends up as chips, compared to 3% for steel. Considering the 24 times less aluminium produced than steel, in absolute terms the total amount of aluminium chips produced is ten times less than steel.

Given the secondary (recycling) CO_2 intensity for aluminium is similar to that of steel (0.43 compared to 0.4 t CO_2/t respectively [115]), equal improvements in chip re-use are likely to yield an approximately ten fold higher CO_2 impact for steel than for aluminium, based on the assumption of replacing recycling with re-use. This equates to between **0.01%** savings of global CO_2 emissions savings for aluminium. However, the primary CO_2 intensity for aluminium is 21.5x that of secondary production, at 8.6 t CO_2/t. Therefore replacing 100% of discarded chips would increase CO_2 savings by a factor of 21.5 to **0.215%** of global CO_2 emissions. It has been estimated that the rate of recycling, i.e. fraction of annual discarded material that becomes part of future production is 39% generally for aluminium [120]. Therefore if this rate is representative of chip recycling rates, a potential CO_2 emissions saving of **0.13%** is predicted. If

we expand the scrap for re-use to include large scrap, the potential saving increases to **0.86%** of global CO_2 emissions. These calculations and assumptions are presented in Figure 23 (d-f).

Mitigating recycling of steel chips in favour of re-use has a larger potential impact on total CO_2 emissions than mitigation of aluminium recycling. Therefore this work puts forward both steel and aluminium re-use as legitimate routes for CO_2 mitigation, however particular attention should be paid to process routes capable of processing steel given the greater potential CO_2 savings associated with its scrap re-use. Although, the perspective of this paper is the contribution of machining waste re-use to CO_2 emission reduction, it is important to understand the practical and economic advantages of this approach. When recycled, machining waste is typically melted into a lower grade of material, lowering its potential value. In addition, the metal yield is typically low, approximately 55% in the case of aluminium [121]. There is also an inevitable reduction in the purity of recycled ingots at the remelting stage [49]. Retaining the composition of machining waste is of great interest given the particularly high value of certain elements. However it should be noted that swarf in some cases is a handling hazard and can auto-ignite in some scenarios, including for both steel and aluminium, with magnesium being the most dangerous. In addition Costs can be as high as $150 per ton to handle and dispose of machining swarf/chips. Machining oils and other combustibles increase the hazardous nature of the swarf/chips and reduce its value by increasing its disposal cost. Convention and practicalities dictate that machining chips tend to be collected together indiscriminately and sold off for recycling or landfilled. There are therefore practical hurdles to overcome to enable machining waste to enter the standard manufacturing process chain.

5. Outlook

This perspective paper has aimed to provide the reader with a basic understanding of chip type material incorporation as well as with an overview of the environmental savings possible. The key processes which have produced successful parts using machining chips of various materials as feedstocks have been captured here. It is clear that the body of work in the field of solid state chip processing is more developed in comparison to melt-based manufacturing techniques, with laser based DED the only direct melt based manufacturing method to have directly used machining chips as a feedstock, according to the literature. This section attempts to link the practicalities of the technology described in section 3, with the ultimate aim of practical implementation under the driver of sustainability.

5.1. Moving from processing of aluminium to steel

Based on the calculations and assumptions in section 4, it is clear that the ability to re-use steel has a particularly large potential global CO_2 saving given its larger contribution to global CO_2 at the primary and secondary production level. However, to date, the majority of research based on chip and swarf re-use has been focused on softer materials, including copper and brass, to aluminium and titanium. This is likely due to the infancy of the processes used for this purpose and the relative ease of initial demonstration of the ability to process chips by using a relatively soft metal. Therefore the ability of the above processes to consolidate harder materials is included in Figure 24 below, along with the hardest

chip material type which has been processed by the respective technique to date. This data is plotted against the chip size appropriate for the technique.

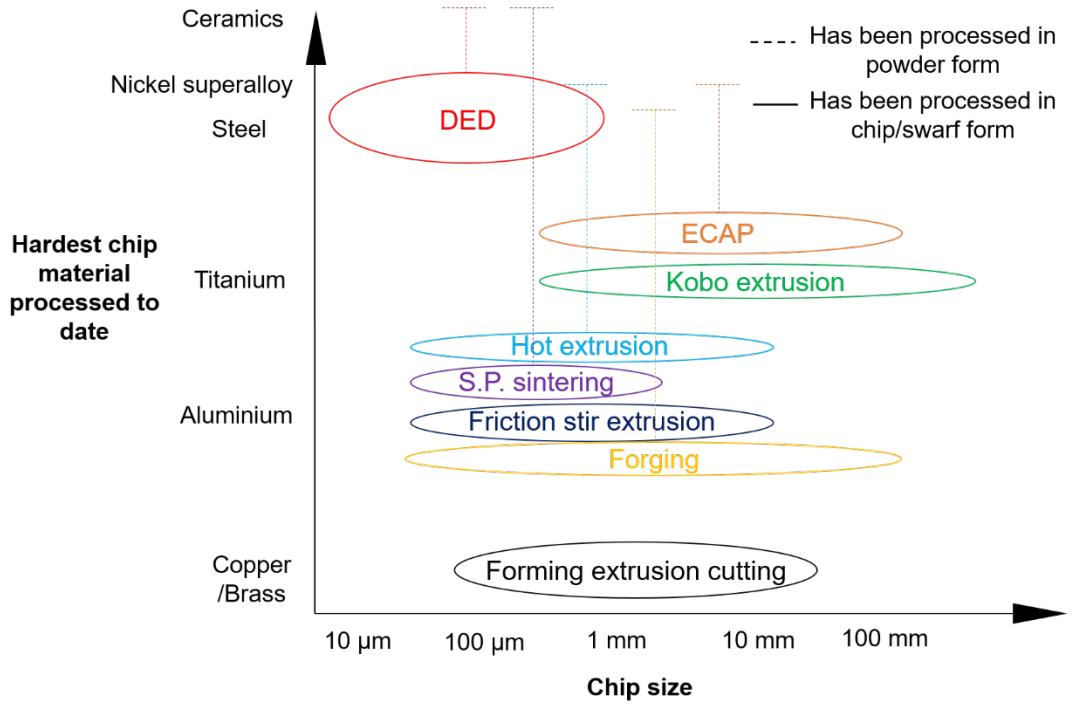


Figure 24 A summary of processes demonstrated to have consolidated machining chips, and indicators of hardest materials which can be consolidated by the processes.

Given the much higher temperatures generated during DED than any of the solid state techniques, the process has the potential to process the hardest materials of all demonstrated chip consolidating processes to date. Materials such as silicon nitride [122] and titanium oxide [123] for example, have been successfully deposited by DED. Machined chips however of such ceramic materials have not yet been processed by laser, although in principle there is no reason why it would not be successful.

Equal channel angular pressing has been demonstrated as a useful technique for pressing ferritic/martensitic [80] and austenitic [124] steels. A nickel single crystal material has also been processed via ECAP for the purpose of grain refinement [125]. Similarly, nickel-base super alloys have been processed by hot extrusion for microstructure control [126,127], and indeed hot extrusion has been used to consolidate steels in powder form [128]. KOBO extrusion is a more niche technique however and has only been demonstrated as useful for titanium chips so far, with harder materials including steel not yet investigated. Hence further experimental proofs of concept may be required to validate the process as suitable for steel machining chips.

Spark plasma sintering is an example a technique used so far to produce parts from aluminium machining chips, however the process itself is capable on consolidating ceramics including SiC [129] and ZnS [130], and the process is appropriate for the consolidation of stainless steel powder [131]. Friction stir extrusion is suited to the processing of aluminium and magnesium materials, and currently there is insufficient evidence to say the process could be scaled to process steel machining chips.

Regarding forging, the process has been used to successfully compact aluminium [91,92] and brass [93] machining chips to date. However, steel powder has been consolidated using forging into dense parts both with [132] or without pre-compaction [133]. Therefore forging can be considered a technology which could be scaled to successfully process steel machining chips. In addition, the large physical scale of forges permits a large range of final products to be potentially produced using this technique. Finally, forming extrusion cutting offers a unique approach for compaction and simultaneous cutting of chips into a grooved, useful shape. To date this has only been demonstrated on copper and brass, and therefore needs further practical investigation to validate the technique for steel or aluminium chips.

A key advantage of the many solid-state approaches to consolidation of machining chips, is their ability to process large swarf and turnings. ECAP, forging and KOBO extrusion have demonstrated their ability to consolidate swarf up to 100s of mm in length. The remaining processes require further investigation of large swarf processing. DED currently suits smaller powders below 1 mm in diameter, however an alternative form of the process can utilise wire being fed beneath the laser, thereby potentially allowing processing of very high aspect ratio swarf with a thin diameter. However further experimental work is required to validate this.

5.2. Summary of consolidation processes

To more conveniently summarise the various techniques which have proven successful at producing dense parts from machining chips, Table 1 summarises all techniques discussed here, along with the material types which have been used successfully, and the drawbacks and benefits of each. This work considers machining chips as a feedstock from the perspective of CO_2 emission savings, and as described in the introduction, steel, and to a lesser degree aluminium are the most important materials consider for waste re-use. For this reason, when steel or aluminium chips have not been the subject of research, a reference to the equivalent powder or other feedstock of steel or aluminium is included, to demonstrate the potential use of each technique for the processing of these materials.

Table 1 Aspects of various prior demonstrated manufacturing processes which can use machining chips. *Italics* denote the material has been processed in powder or other form, but not from chip form.

	Materials and parameters	**Drawbacks**	**Benefits**
	Solid state		
Hot extrusion	Aluminium chips, 500-550°C [48] Aluminium-silicon alloy milling swarf and lathe turnings [49] *Steel powder* [128]	Chips granulated, cleaned beforehand [48] Compaction performed beforehand [48] [49] Milling swarf superior to lathe turnings, in bonding, density and UTS [49]. Sensitivity to chip size Inferior mechanical properties to parent material [49]. Non-continuous process	95%+ material usage [48] 97%+ density [48]

KOBO extrusion	Titanium swarf, dry machined [55] 350°C used [55] *Aluminium rod used* [134]	Compaction performed beforehand [55]	Can use very large swarf (100-200 mm length x 0.3 x 2.5 mm) [55] Can process less formable materials (e.g. Ti) High density, mechanical properties close to original material [55] Fine, uniform grain structure produced [55]
Friction stir extrusion	Aluminium chips [65] [64] Magnesium alloy chips [69] Aluminium chips with added SiC powder [71]	Compaction performed beforehand [65] Density better in thin wire than bulk parts [83]	Continuous (mixed results) [70] Can be used to produce composites with added powder [71] Energy efficiency better than ECAP [72]
Forming /Ploughing extrusion cutting	Copper chips [75,135]	Only used so far to produce grooved strips [75]	Continuous process High density
Spark plasma sintering	Magnesium/magnesium alloy chips 500°C, 33 MPa [96] Aluminium chips mixed with aluminium powder [98] at 490°C *Steel powder used* [136]	Chips acetone cleaned beforehand [96] Compaction performed beforehand [96] Limited size of parts Non-continuous process	High density achieved, porosity similar to that of casting ingots [96] Chip surface oxides fragmented by SPS [96] Fine microstructure due to machining is maintained after SPS [96] Increased ultimate tensile strength compared to parent material [96]
Equal channel angular pressing	Titanium 450°C [67], Ti-6Al-4V chips [69] *Steel billets used* [61] *Aluminium billets used* [137]	Dry milling used [85] Non-continuous process	Full density achieved [85] Strength comparable or better than that from ingot or powder Ti. [85] Surface oxides fragmented [85]
Forging	Aluminium chips, 480°C, 120 mins process time [91] Brass [93] Aluminium 6061 [92] *Steel powder used with* [132] *or without pre-compaction* [133]	Aluminium chips needed pre-heating/softening before compaction [91] [92] Brass [93], required pre-compaction	Large chip size shows best UTS [91] Density highly dependent on initial chip size, small chips best [92]
	Melt based		

Directed energy deposition	Inconel 617 chips used after ball milling [106] Ti-6Al-4V chips used after ball milling [109] Carbon steel chips sieved [104] *Aluminium powder used* [138]	Cannot use very large turnings as feedstock currently. Hard limit to the particle size processable.	High temperature, melts all metal, some ceramics Chips up to 418 μm melted into dense tracks. Beyond this size not investigated. Continuous process

So far, in the vast majority of the work considering use of machining chips for re-use, both the solid state or melt-based methods, the chips have been cleaned of machining coolant fluid after production, or produced under dry machining conditions. This is to avoid unwanted contamination in parts which may otherwise match in mechanical properties those of the parent material from which the chips were made. However many of these processes, being at high temperatures, may be able to fragment and disperse contaminants during the process, and such phenomena should be investigated to avoid an unnecessary cleaning stuff. Nevertheless, with other methods for producing clean chips as presented in this paper, including cryogenic machining and ultrasonic dry machining, there is significant potential for production of clean chips while maintaining good machining rates and low tool wear rates, in practical scenarios. Hence, future experimental research should incorporate such techniques in a high efficiency process chain.

The constraint of chip size on the ability of the re-use manufacturing process to work efficiently differs for solid-state and melt-based processes. Many of the solid-state processes can readily use or even benefit from chips with large size. KOBO extrusion for example can densify swarf up to 200 mm in length. However, DED is fundamentally limited in feedstock size processable, depending on the size of the laser spot. For this reason, the end-use of chips bound for re-use is critically dependent on size distribution (as well as cleanliness, form and composition).

As shown in Table 1, academic work so far on solid-state re-use has mostly been bound to more malleable materials such as aluminium and magnesium, and sometimes titanium alloys. As a proof of concept it is expected that more readily deformable materials have been the focus of the research. However, for all processes except KOBO extrusion and ploughing extrusion cutting, steel powder or billet feedstock have been used previously successfully, and hence machining chips of steel are likely to be successfully processed by these techniques. This is expected to be the subject of future work in these processes. DED however, owing to its high melting point and relative insensitivity to powder size and properties in its ability to process materials, has been successfully used to deposit the harder steel and nickel based materials and is therefore a proven appropriate technique for this form of re-use. The insensitivity of DED to feedstock size is a strong selling point for its application to machining chip use. In particular, within a certain size range, significant variation in morphology is unlikely to play a large role in the ability of chips to be melted and deposited. This is a major driving factor for the potential role of DED in the chip re-use space.

5.3. Process chain choice

There are several distinct forms of machining chip which may be produced from a machining operation. These chips may differ by the level of coolant remaining on the chip surface, or level of contamination or oxidation. The size and morphology may also vary significantly. These variations of chip properties inform the choice of process route to be selected for direct re-use. To summarise the process chains which have proved possible according to the literature, a schematic showing chip production and example end-use processes, is shown in Figure 25.

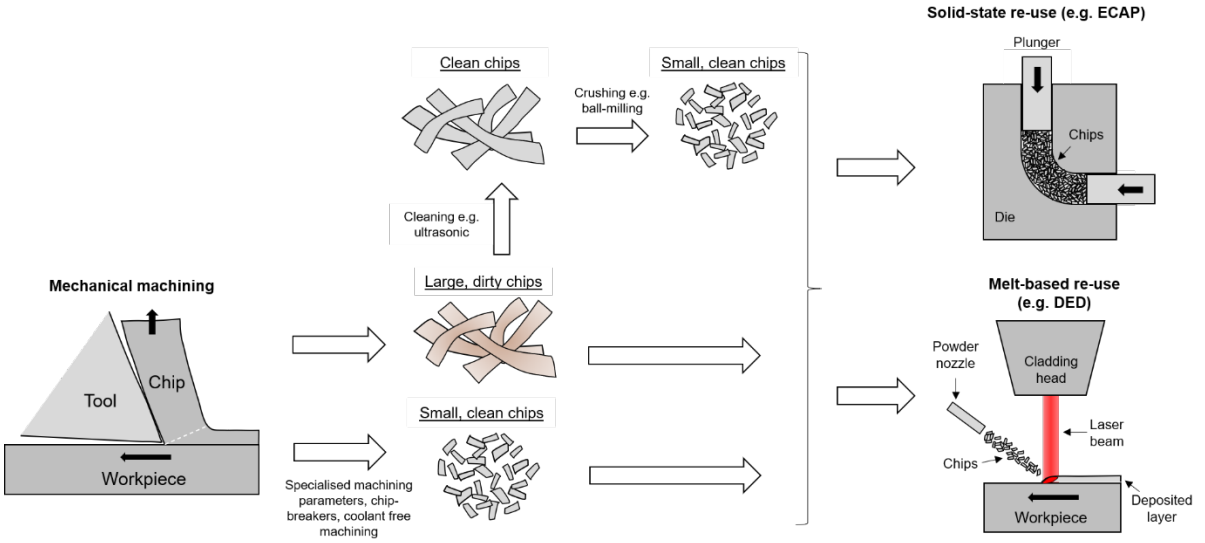


Figure 25 Schematic showing the routes for re-use of machining chips with and without further processing prior to re-use.

In this schematic, three example post-processing options for machining chips produced under typical industrial conditions with coolant, are proposed. One approach is the design of the machining process to operate under dry conditions using revamped machining conditions, or using a cryogenic fluid such as LN2, as well as modified cutting parameters to yield finer particles. In this scenario, the chips are versatile and can be used for all potential re-use techniques described in Table 1. Another scenario is the production of clean chips via an ultrasonic method after machining, followed by a process such as ball-milling to yield an appropriate controlled chip size. However in this case the efficiency and practicality of these post-processing techniques should be carefully considered. In the third case, the contaminated machining chips are used in the re-use process, and the final part produced from such a feedstock is used solely in situations where the sacrificed mechanical and microstructural properties can be tolerated. Areas for innovation in chip generation therefore include and can be summarised as – cleaner chips, better shaped chips, more consistent chips, and purer chips.

In summary, there are several options available to manufacturers who are interested in re-use of in-house made machining scrap for both economic and environmental purposes. Critically, the process chain choice depends on the intended properties of the final consolidated product. Here it is proposed obtaining simple, consolidated material is straight forward and does not require significant chip processing. However further research is required to understand the fundamental impact of chip contamination on the properties of parts made via both solid state and melt based methods.

5.4. Accessing larger scrap – the automotive industry case

To understand the importance of metal sheet producing technology, it can be noted that approximately 50% of annual global production of liquid metal is used to make sheets, and around half of this does not reach a final product but is instead scrapped and recycled [139,140]. A significant source of scrap is during blanking, where coils of strip metal are cut into shapes for forming further downstream. Poor tessellation between these shapes results in significant scrappage of wasted material [139].

Metal stamping is the most important metal processing technique for automotive body-in-white manufacturing. Most automobiles have between 100-150 stamped metal parts, from small brackets to large panels including hoods and body sides [141]. Horton & Allwood, using an anonymous manufacturer case study, gave some example utilisation rates on various parts of the body in white production process [142]. More intricate parts yielded lower utilisation rates, for example with the "body side" yielding only 32% utilisation, and the "fender outer" part yielding 26%. The "front door outer" however, as a simpler, more geometrically simple part, yielded a much higher 68% utilisation.

In Figure 25, it is shown that after construction, using the UK as an example, the automotive industry produces the largest amount of steel scrap. The CO_2 savings proposed in section 1 are based upon an estimation of "small" scrap types which can be readily be re-used as feedstock for manufacturing processes. Accessing steel scrap produced through automotive manufacturing alone, is worth 18.5% of UK manufacturing scrap, in comparison to the estimated 10% in small form or machining chips. Therefore the potential savings in terms of steel will almost triple if we can access this form of scrap from body-in-white production for direct re-use. In addition, incorporating end of life car scrap to this will enhance this saving. It has been predicted that 12% of steel and 30% of aluminium produced globally is used in the automotive industry, one third of which is in the form of sheet metal [6]. Cullen et al. determine that global automotive sheet metal yield losses for steel are 40% [140]. A flowchart illustrating these process chains is shown in Figure 26.

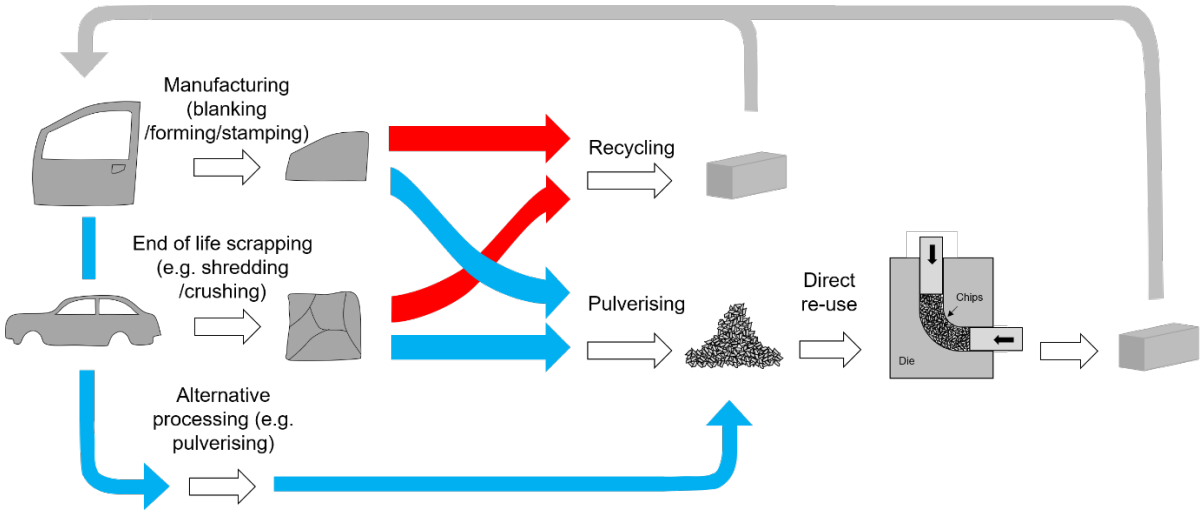


Figure 26 Proposed alternative approach to handling of automotive scrap, both at the manufacturing and end-of-life stage. Pulverising of large scrap is proposed as a sensible approach to avoid unnecessary recycling related emissions.

Both manufacturing scrap (representing e.g. 5.7% of all UK steel) and end of life automotive scrap offer a substantial source of steel which can be diverted from recycling to re-use, and in this way mitigate the CO_2 emissions associated with recycling.

There are two approaches which offer the potential to avoid recycling and produce material ready for direct re-use: (1) changing current manufacturing process – e.g. changing some blanking processes to milling or turning, or (2) adding new manufacturing processes e.g. pulverising or milling of scrap. The former approach offers the greatest benefit in overall emission mitigation, as there is no added process to the system, thereby avoiding large additional energy costs. The second approach offers the advantage of not requiring a costly change to the manufacturing system, however will incur an additional energy and CO_2 emission cost associated with further processing.

5.5. Opportunities and barriers

The end-goal for chip generation, in the context of re-usability, is that chip size can be reduced, without compromising the efficiency of the machining operation, in the absence of contamination. These chips may be densely packed, transportable and flexible in terms machining operation for which they can be a feedstock material. Machining technology has advanced significantly, and new and emergent technologies, some of which have been identified in this work, can not only enhance the machining operation but can create a more re-usable waste product. In product applications requiring narrow windows of part properties, the presence of machining coolants presents a challenge, however combinations of techniques including minimum quantity/aerosol lubricants and cryogenic machining, along with chip cleaning offer clear and practical solutions. However the “prize” of solving the ideal chip problem is significant compared to the state of the current route with modest improvements to technology. The authors propose that waste streams should be designed from the beginning of manufacturing process chains which involve machining, integrating chip management systems, logging cleanliness and origin of each chip type. There is a current bias in the state-of-the-art in chip re-use for titanium alloy re-use – explained by its high value and relatively high mass of chips produced per kg of final machined part, for example in the aerospace sector. This work proposes that iron and aluminium based waste streams become the focus of chip re-use efforts, given their much greater contributions to global CO_2 emissions.

Acknowledgements

This work was funded by the EPSRC project UK FIRES: Locating Resource Efficiency at the heart of Future Industrial Strategy in the UK (ref. EP/S019111/1).

References

[1] Samuel M. A new technique for recycling aluminium scrap. Journal of Materials Processing Technology 2003;135:117–24. doi:10.1016/S0924-0136(02)01133-0.

[2] Cullen JM, Allwood JM. Mapping the global flow of aluminum: From liquid aluminum to end-use goods. Environmental science & technology. 2013; 47(7):3057-64.

doi:10.1021/es304256s.

[3] Allwood JM, Dunant CF, Lupton RC, Cleaver CJ, Serrenho ACH, Azevedo JMC, et al. Absolute Zero: Delivering the UK's climate change commitment with incremental changes to today's technologies. 2019. doi:10.17863/CAM.46075.

[4] IEA. Energy Technology Perspectives 2016 – Analysis - IEA 2016.

[5] Commision ET. Reaching zero carbon emissions from Steel. 2018.

[6] Allwood J. Sustainable materials-with both eyes open THE FUTURE IN PRACTICE THE STATE OF SUSTAINABILITY LEADERSHIP. 2012.

[7] Cooper DR. Reuse of steel and aluminium without melting. University of Cambridge, 2014. doi:https://doi.org/10.17863/CAM.14065.

[8] Luo Z, Soria A. Prospective Study of the World Aluminium Industry. JRC Scientific and Technical Reports 2007. doi:10.2791/36024.

[9] International Aluminium Institute. Aluminium for Future Generations/2008 update. 2008.

[10] Global Industry Analysts Inc. Steel Scrap - Global Strategic Business Report. 2024.

[11] Li P, Li X, Li F, A novel recycling and reuse method of iron scraps from machining process. Journal of cleaner production, 266, p.121732. 2020. doi:10.1016/j.jclepro.2020.121732.

[12] Allwood JM, Cullen JM, Cooper DR, Milford RL, Patel ACH, Carruth MA, McBrien M. Conserving our metal energy: Avoiding melting steel and aluminium scrap to save energy and carbon. 2010.

[13] Wan B, Chen W, Lu T, Liu F, Jiang Z, Mao M. Review of solid state recycling of aluminum chips. Resources, Conservation and Recycling. 2017; 125:37-47. doi:10.1016/j.resconrec.2017.06.004.

[14] Childs TH, Arrazola PJ, Azpitarte L, Garay A, Soriano D, Mikel S, Cuesta M, Physical modelling with experimental validation of high ductility metal cutting chip formation illustrated by copper machining. International Journal of Machine Tools and Manufacture, 2022; 173, p.103847. doi: 10.1016/j.ijmachtools.2021.103847.

[15] Yılmaz B, Karabulut Ş, Güllü A. A review of the chip breaking methods for continuous chips in turning. Journal of Manufacturing Processes 2020;49:50–69. doi:10.1016/j.jmapro.2019.10.026.

[16] Lotfi M, Farid AA, Soleimanimehr H. A new hybrid model based on the radius ratio for prediction of effective cutting limit of chip breakers. J Engineering Manufacture 2016;230:1417–27. doi:10.1177/0954405415586549.

[17] Palaniappan K, Sundararaman M, Murthy H, Jeyaraam R, Rao, BC, Influence of workpiece texture and strain hardening on chip formation during machining of Ti–6Al–4V alloy. International Journal of Machine Tools and Manufacture, 2022; 173, p.103849. doi:10.1016/j.ijmachtools.2021.103849.

[18] Chau SY, To S, Sun Z, Wu H. Twinned-serrated chip formation with minor shear bands in ultra-precision micro-cutting of bulk metallic glass. International Journal of Advanced Manufacturing Technology 2020;107:4437–48. doi:10.1007/s00170-020-04977-9.

[19] Haddag B, Atlati S, Nouari M, Moufki A. Dry machining aeronautical aluminum alloy AA2024-T351: Analysis of cutting forces, chip segmentation and built-up edge formation. Metals 2016;6. doi:10.3390/met6090197.

[20] Haddag B, Makich H, Nouari M, Dhers J. Tribological behaviour and tool wear analyses in rough turning of large-scale parts of nuclear power plants using grooved coated insert 2014. doi:10.1016/j.triboint.2014.06.017.

[21] Miyazawa H, Takeuchi S, Miyake S, Murakawa M. Sintered diamond cutting inserts with chip breaker prepared by laser technique. vol. 86. 1996.

[22] Degenhardt JA, Devor RE, Kapoor SG. Generalized groove-type chip breaker effects on drilling for different drill diameters and flute shapes 2005. doi:10.1016/j.ijmachtools.2005.02.009.

[23] Issahaq MN, Udupa A, Saei M, Mohanty DP, Mann JB, Sundaram NK, Trumble KP, Chandrasekar S. Dual-scale folding in cutting of commercially pure aluminum alloys. International Journal of Machine Tools and Manufacture, 2022; 181, p.103932. doi:10.1016/j.ijmachtools.2022.103932.

[24] Zhang XP, Wu SB. Chip control in the dry machining of hardened AISI 1045 steel. The International Journal of Advanced Manufacturing Technology. 2017;88:3319-27. doi:10.1007/s00170-016-8989-2.

[25] Słodki B, Zębala W, Struzikiewicz G. Correlation Between Cutting Data Selection and Chip Form in Stainless Steel Turning. Machining Science and Technology 2015;19:217–35. doi:10.1080/10910344.2015.1018530.

[26] Goindi GS, Sarkar P. Dry machining: A step towards sustainable machining e Challenges and future directions 2017. doi:10.1016/j.jclepro.2017.07.235.

[27] Tan R, Zhao X, Guo S, Zou X, He Y, Geng Y, et al. Sustainable production of dry-ultra-precision machining of Tie6Ale4V alloy using PCD tool under ultrasonic elliptical vibration-assisted cutting 2019. doi:10.1016/j.jclepro.2019.119254.

[28] Liang X, Zhang C, Cheung CF, Wang C, Li K, Bulla B. Micro/nano incremental material removal mechanisms in high-frequency ultrasonic vibration-assisted cutting of 316L stainless steel.

International Journal of Machine Tools and Manufacture. 2023;191:104064. doi:10.1016/j.ijmachtools.2023.104064.

[29] Weinert K, Inasaki I, Sutherland JW, Wakabayashi T. Dry machining and minimum quantity lubrication. CIRP Annals - Manufacturing Technology 2004;53:511–37. doi:10.1016/S0007-8506(07)60027-4.

[30] Hong SY, Ding Y, Ekkens RG. Improving low carbon steel chip breakability by cryogenic chip cooling. vol. 39. 1999.

[31] Sampaio MA, Machado ÁR, Laurindo CA, Torres RD, Amorim FL. Influence of minimum quantity of lubrication (MQL) when turning hardened SAE 1045 steel: a comparison with dry machining. The International Journal of Advanced Manufacturing Technology. 2018; 98:959-68. doi:10.1007/s00170-018-2342-x.

[32] Wang W, Wang B, Liu B, Gao H, Wei Z. Machinability and chip morphology evolution of hardened stainless steel using liquid nitrogen cryogenic. The International Journal of Advanced Manufacturing Technology. 2023; 125(1):967-87. doi:10.1007/s00170-022-10765-4.

[33] Yıldırım ÇV, Kıvak T, Sarıkaya M, Şirin Ş. Evaluation of tool wear, surface roughness/topography and chip morphology when machining of Ni-based alloy 625 under MQL, cryogenic cooling and CryoMQL. Journal of Materials Research and Technology. 2020; 9(2):2079-92. doi:10.1016/j.jmrt.2019.12.069.

[34] Furukawa M, Horita Z, Nemoto M, Langdon TG. The use of severe plastic deformation for microstructural control. vol. 324. 2002.

[35] Kanani M, Sohrabi S, Ebrahimi R, Paydar MH. Continuous and ultra-fine grained chip production with large strain machining. Journal of Materials Processing Technology 2014;214:1777–86. doi:10.1016/j.jmatprotec.2014.03.028.

[36] Yang X, Zhang B, Bai Q, Zheng M, Tang J. Grain size influence on chip formation in high-speed machining of pure iron. International Journal of Advanced Manufacturing Technology 2020;108:1357–66. doi:10.1007/s00170-020-05512-6.

[37] Courbon C, Mabrouki T, Rech J, Mazuyer D, Perrard F, D'eramo E. Further insight into the chip formation of ferritic-pearlitic steels: Microstructural evolutions and associated thermo-mechanical loadings. International Journal of Machine Tools and Manufacture. 2014; 77:34-46. doi:10.1016/j.ijmachtools.2013.10.010.

[38] El Baradie MA. Cutting fluids: Part I. Characterisation. Journal of Materials Processing Technology 1996;56:786–97. doi:10.1016/0924-0136(95)01892-1.

[39] Abbá E, Speidel A, Liao Z, Axinte D, Novovic D. A bar of cutting fluid: Deep Eutectic Fluids with a novel flavour. Materials Today Advances. 2022; 16:100291. doi: 10.1016/j.mtadv.2022.100291.

[40] Lee C-M, Choi Y-H, Ha J-H, Woo W-S. Eco-Friendly Technology for Recycling of Cutting Fluids and Metal Chips: A Review. International Journal of Precision Engineering and Manufacturing – Green Technology. 2017;4:457. doi:10.1007/s40684-017-0051-9.

[41] Cambiella A, Benito JM, Pazos C, Coca J. Centrifugal separation efficiency in the treatment of waste emulsified oils. Chemical Engineering Research and Design 2006;84:69–76. doi:10.1205/cherd.05130.

[42] Rahaman MN. Kinetics and mechanisms of densification. Sintering of Advanced Materials, Elsevier; 2010, p. 33–64. doi:10.1533/9781845699949.1.33.

[43] Zhang C, Li H, Li & MQ, Li MQ. Formation mechanisms of high quality diffusion bonded martensitic stainless steel joints. Science and Technology of Welding and Joining 2014;20:115–22. doi:10.1179/1362171814Y.0000000258.

[44] Yu J, Zhao G. Interfacial structure and bonding mechanism of weld seams during porthole die extrusion of aluminum alloy profiles 2018. doi:10.1016/j.matchar.2018.01.052.

[45] Shirzadi AA, Assadi H, Wallach ER. Interface evolution and bond strength when diffusion bonding materials with stable oxide films. 2001.

[46] Luo P, Mcdonald DT, Xu W, Palanisamy S, Dargusch MS, Xia K. A modified Hall-Petch relationship in ultrafine-grained titanium recycled from chips by equal channel angular pressing 2012. doi:10.1016/j.scriptamat.2012.02.008.

[47] Gronostajski JZ, Marciniak H, Matuszak A. Production of composites on the base of AlCu4 alloy chips. vol. 60. 1996.

[48] Gronostajski J, Matuszak A. Recycling of metals by plastic deformation: an example of recycling of aluminium and its alloys chips. Journal of Materials Processing Technology 1999;92–93:35–41. doi:10.1016/S0924-0136(99)00166-1.

[49] Chiba R, Yoshimura M. Solid-state recycling of aluminium alloy swarf into c-channel by hot extrusion. Journal of Manufacturing Processes 2015;17:1–8. doi:10.1016/j.jmapro.2014.10.002.

[50] Kolpak F, Schulze A, Dahnke C, Tekkaya AE. Predicting weld-quality in direct hot extrusion of aluminium chips 2019. doi:10.1016/j.jmatprotec.2019.116294.

[51] Güley V, Güzel A, Jäger A, Khalifa N Ben, Tekkaya AE, Misiolek WZ. Effect of die design on the welding quality during solid state recycling of AA6060 chips by hot extrusion 2013. doi:10.1016/j.msea.2013.03.010.

[52] Chiba R, Nakamura T, Kuroda M. Solid-state recycling of aluminium alloy swarf through cold profile extrusion and cold rolling. Journal of Materials Processing Technology 2011;211:1878–87. doi:10.1016/j.jmatprotec.2011.06.010.

[53] Schulze A, Hering O, Tekkaya AE. Production and subsequent forming of chip-based aluminium sheets without remelting. International Journal of Precision Engineering and Manufacturing-Green Technology. 2022; 9(4):1035-48. doi: 10.1007/s40684-021-00395-8.

[54] Laurent-Brocq M, Lilensten L, Pinot C, Schulze A, Duchaussoy A, Bourgon J, Leroy E, Tekkaya AE. Solid state recycling of aluminium chips: Multi-technique characterization and analysis of oxidation. Materialia. 2023; 31:101864. doi: 10.1016/j.mtla.2023.101864.

[55] Topolski K, Bochniak W, Łagoda M, Ostachowski Pawełand Garbacz H. Structure and properties of titanium produced by a new method of chip recycling. Journal of Materials Processing Technology 2017;248:80–91. doi:10.1016/j.jmatprotec.2017.05.005.

[56] Güley V, Khalifa N Ben, Tekkaya AE. Direct Recycling of 1050 Aluminum Alloy Scrap Material Mixed with 6000 Aluminum Alloy Chips by Hot Extrusion. International Journal of Material Forming. 2010; doi:10.1007/s12289-010-0904-z.

[57] Korbel A, Bochniak W. Refinement and control of the metal structure elements by plastic deformation. Scripta Materialia 2004;51:755–9. doi:10.1016/j.scriptamat.2004.06.020.

[58] Widerøe F, Welo T. Using contrast material techniques to determine metal flow in screw extrusion of aluminium. Journal of Materials Processing Technology. 2013; 213(7):1007-18. doi: 10.1016/j.jmatprotec.2012.11.013.

[59] Whalen S, Overman N, Taysom BS, Bowden M, Reza-E-Rabby M, Skszek T, DiCiano M. Effect of high iron content on direct recycling of unhomogenized aluminum 6063 scrap by Shear Assisted Processing and Extrusion. Journal of Manufacturing Processes. 2023; 97:115-24. doi: 10.1016/j.jmapro.2023.04.067.

[60] Whalen S, Taysom BS, Overman N, Reza-E-Rabby M, Qiao Y, Richter T, Skszek T, DiCiano M. Porthole die extrusion of aluminum 6063 industrial scrap by shear assisted processing and extrusion. Manufacturing Letters. 2023; 36:52-6. doi:10.1016/j.mfglet.2023.01.005.

[61] Sakow S, Tokunaga T, Ohno M, Matsuura K. Microstructure refinement and mechanical properties improvement of Al-Si-Fe alloys by hot extrusion using a specially designed high-strain die 2019. doi:10.1016/j.jmatprotec.2019.116447.

[62] Lin J, Wang X, Ren W, Yang X, Wang Q. Enhanced Strength and Ductility Due to Microstructure Refinement and Texture Weakening of the GW102K Alloy by Cyclic Extrusion Compression 2016. doi:10.1016/j.jmst.2016.01.004.

[63] Whalen S, Olszta M, Roach C, Darsell J, Graff D, Reza-E-Rabby M, et al. High ductility aluminum alloy made from powder by friction extrusion. Materialia 2019;6:100260. doi:10.1016/j.mtla.2019.100260.

[64] Tang W, Reynolds AP. Production of wire via friction extrusion of aluminum alloy machining chips. Journal of Materials Processing Technology 2010;210:2231–7.

doi:10.1016/j.jmatprotec.2010.08.010.

[65] Mehtedi M El, Forcellese A, Mancia T, Simoncini M, Spigarelli S. A new sustainable direct solid state recycling of AA1090 aluminum alloy chips by means of friction stir back extrusion process. Procedia CIRP, vol. 79, Elsevier B.V.; 2019, p. 638–43. doi:10.1016/j.procir.2019.02.062.

[66] Li X, Baffari D, Reynolds AP. Friction stir consolidation of aluminum machining chips. The International Journal of Advanced Manufacturing Technology. 2018; 94:2031-42. doi:10.1007/s00170-017-1016-4.

[67] Latif A, Ingarao G, Fratini L. Multi-material based functionally graded billets manufacturing through friction stir consolidation of aluminium alloys chips. CIRP Annals. 2022; 71(1):261-4. doi: 10.1016/j.cirp.2022.03.035.

[68] Puleo R, Latif A, Ingarao G, Di Lorenzo R, Fratini L. Solid bonding criteria design for aluminum chips recycling through Friction Stir Consolidation. Journal of Materials Processing Technology. 2023; 319:118080. doi:10.1016/j.jmatprotec.2023.118080.

[69] Baffari D, Buffa G, Campanella D, Fratini L, Reynolds AP. Process mechanics in Friction Stir Extrusion of magnesium alloys chips through experiments and numerical simulation. Journal of Manufacturing Processes 2017;29:41–9. doi:10.1016/j.jmapro.2017.07.010.

[70] Baffari D, Buffa G, Campanella D, Fratini L. Design of continuous Friction Stir Extrusion machines for metal chip recycling: Issues and difficulties. Procedia Manufacturing, vol. 15, Elsevier B.V.; 2018, p. 280–6. doi:10.1016/j.promfg.2018.07.220.

[71] Baffari D, Buffa G, Campanella D, Fratini L. Al-SiC Metal Matrix Composite production through Friction Stir Extrusion of aluminum chips. Procedia Engineering, vol. 207, Elsevier Ltd; 2017, p. 419–24. doi:10.1016/j.proeng.2017.10.798.

[72] Baffari D, Reynolds AP, Masnata A, Fratini L, Ingarao G. Friction stir extrusion to recycle aluminum alloys scraps: Energy efficiency characterization. Journal of Manufacturing Processes 2019;43:63–9. doi:10.1016/j.jmapro.2019.03.049.

[73] Borgert T, Homberg W. Analysis of temperature effect on strength and microstructure in friction induced recycling process (FIRP). Materials Research Proceedings. 2023; 28. doi:10.21741/9781644902479-211.

[74] De Chiffre L. Extrusion cutting of brass strips. International Journal of Machine Tool Design and Research 1983;23:141–51. doi:10.1016/0020-7357(83)90013-6.

[75] Zhang J, Pang X, Chen H, Shi G, Deng W. Process and forming performance of ploughing extrusion cutting for recycling of metal chips. Journal of Materials Processing Technology 2019;274:116283. doi:10.1016/j.jmatprotec.2019.116283.

[76] Shi Q, Tse YY, Higginson RL. Microstructure and texture development during solid

consolidation recycling of Ti-6Al-4V 2018. doi:10.1016/j.matchar.2018.10.020.

[77] Kim WJ, Chung CS, Ma DS, Hong SI, Kim HK. Optimization of strength and ductility of 2024 Al by equal channel angular pressing (ECAP) and post-ECAP aging. Scripta Materialia 2003;49:333–8. doi:10.1016/S1359-6462(03)00260-4.

[78] Razavi SM, Foley DC, Karaman I, Hartwig KT, Duygulu O, Kecskes LJ, et al. Effect of grain size on prismatic slip in Mg-3Al-1Zn alloy. Scripta Materialia 2012;67:439–42. doi:10.1016/j.scriptamat.2012.05.017.

[79] Vaughan MW, Samimi P, Gibbons SL, Abrahams RA, Harris RC, Barber RE, et al. Exploring performance limits of a new martensitic high strength steel by ausforming via equal channel angular pressing. Scripta Materialia 2020;184:63–9. doi:10.1016/j.scriptamat.2020.03.011.

[80] Islamgaliev RK, Nikitina MA, Ganeev A V, Sitdikov VD. Strengthening mechanisms in ultrafine-grained ferritic/martensitic steel produced by equal channel angular pressing 2018. doi:10.1016/j.msea.2018.11.141.

[81] Gibbons SL, Abrahams RA, Vaughan MW, Barber RE, Harris RC, Arroyave R, et al. Microstructural refinement in an ultra-high strength martensitic steel via equal channel angular pressing. Materials Science and Engineering A 2018;725:57–64. doi:10.1016/j.msea.2018.04.005.

[82] Bhadeshia HKDH, Harada H. High-strength (5 GPa) steel wire: an atom-probe study. Applied Surface Science 1993;67:328–33. doi:10.1016/0169-4332(93)90334-8.

[83] Tomota Y, Suzuki T, Kanie A, Shiota Y, Uno M, Moriai A, et al. In situ neutron diffraction of heavily drawn steel wires with ultra-high strength under tensile loading. Acta Materialia 2005;53:463–7. doi:10.1016/j.actamat.2004.10.003.

[84] Haase M, Khalifa N Ben, Tekkaya AE, Misiolek WZ. Improving mechanical properties of chip-based aluminum extrudates by integrated extrusion and equal channel angular pressing (iECAP). Materials Science and Engineering A 2012;539:194–204. doi:10.1016/j.msea.2012.01.081.

[85] Luo P, Xie • H, Paladugu • M, Palanisamy • S, Dargusch • M S, Xia • K. Recycling of titanium machining chips by severe plastic deformation consolidation. Journal of Materials Science 2010. doi:10.1007/s10853-010-4443-2.

[86] Shi Q. Recycling of Titanium Alloys from Machining Chips using Equal Channel Angular Pressing. 2015.

[87] Shi Q, Tse YY, Higginson RL. Effects of processing parameters on relative density, microhardness and microstructure of recycled Ti-6Al-4V from machining chips produced by equal channel angular pressing. Materials Science and Engineering A 2016;651:248–58. doi:10.1016/j.msea.2015.11.002.

[88] Xu C, Furukawa M, Horita Z, Langdon TG. The evolution of homogeneity and grain refinement during equal-channel angular pressing: A model for grain refinement in ECAP. Materials Science and Engineering A 2005;398:66–76. doi:10.1016/j.msea.2005.03.083.

[89] Luo P, McDonald DT, Zhu SM, Palanisamy S, Dargusch MS, Xia K. Analysis of microstructure and strengthening in pure titanium recycled from machining chips by equal channel angular pressing using electron backscatter diffraction. Materials Science and Engineering A 2012;538:252–8. doi:10.1016/j.msea.2012.01.039.

[90] Zhan M, Sun Z, Yang H. Modeling of Hot Forging. Comprehensive Materials Processing, vol. 5, Elsevier Ltd; 2014, p. 441–93. doi:10.1016/B978-0-08-096532-1.00529-X.

[91] Khamis SS, Lajis MA, Albert RAO. A sustainable direct recycling of aluminum chip (AA6061) in hot press forging employing Response surface methodology. Procedia CIRP, vol. 26, Elsevier B.V.; 2015, p. 477–81. doi:10.1016/j.procir.2014.07.023.

[92] Shahrom MS, Yusoff AR. Cyclic extrusion compression back pressure technique for hot forging process in direct recycling of aluminium 6061 machining chip. Journal of Manufacturing Processes 2017;29:1–9. doi:10.1016/j.jmapro.2017.07.003.

[93] Johansson J, Ivarsson L, Ståhl JE, Bushlya V, Schultheiss F. Hot Forging Operations of Brass Chips for Material Reclamation after Machining Operations. Procedia Manufacturing 2017;11:584–92. doi:10.1016/j.promfg.2017.07.152.

[94] Guillon O, Gonzalez-Julian J, Dargatz B, Kessel T, Schierning G, Räthel J, et al. Field-Assisted Sintering Technology/Spark Plasma Sintering: Mechanisms, Materials, and Technology Developments. Advanced Engineering Materials 2014;16:830–49. doi:10.1002/adem.201300409.

[95] Anselmi-Tamburini U. Spark Plasma Sintering. Encyclopedia of Materials: Technical Ceramics and Glasses, Elsevier; 2021, p. 294–310. doi:10.1016/b978-0-12-803581-8.11730-8.

[96] Paraskevas D, Dadbakhsh S, Vleugels J, Vanmeensel K, Dewulf W, Duflou JR. Solid state recycling of pure Mg and AZ31 Mg machining chips via spark plasma sintering 2016. doi:10.1016/j.matdes.2016.07.082.

[97] Groza JR, Zavaliangos A. Sintering activation by external electrical field. Materials Science and Engineering A 2000;287:171–7. doi:10.1016/s0921-5093(00)00771-1.

[98] Paraskevas D, Vanmeensel K, Vleugels J, Dewulf W, Duflou JR. The use of Spark Plasma Sintering to fabricate a two-phase material from blended aluminium alloy scrap and gas atomized powder. Procedia CIRP, vol. 26, Elsevier B.V.; 2015, p. 455–60. doi:10.1016/j.procir.2014.07.074.

[99] Calvert JR. Microstructure and mechanical properties of WE43 alloy produced via additive friction stir technology. Doctoral dissertation, Virginia Tech; 2015.

[100] Jordon JB, Allison PG, Phillips BJ, Avery DZ, Kinser RP, Brewer LN, Cox C, Doherty K. Direct recycling of machine chips through a novel solid-state additive manufacturing process. Materials & Design. 2020;193:108850. doi:10.1016/j.matdes.2020.108850.

[101] Agrawal P, Haridas RS, Yadav S, Thapliyal S, Gaddam S, Verma R, Mishra RS. Processing-structure-property correlation in additive friction stir deposited Ti-6Al-4V alloy from recycled metal chips. Additive Manufacturing. 2021; 47:102259. doi:10.1016/j.addma.2021.102259.

[102] Prasad HS, Brueckner F, Kaplan AFH. Powder catchment in laser metal deposition. J Laser Appl 2019;31:22308. doi:10.2351/1.5096130.

[103] Siva Prasad H, Brueckner F, Kaplan AFH. Powder incorporation and spatter formation in high deposition rate blown powder directed energy deposition. Additive Manufacturing 2020;35:101413. doi:10.1016/j.addma.2020.101413.

[104] Mahmood K, Syed WUH, Pinkerton AJ. Innovative reconsolidation of carbon steel machining swarf by laser metal deposition. Optics and Lasers in Engineering 2011;49:240–7. doi:10.1016/j.optlaseng.2010.09.014.

[105] Hofmeister W, Griffith M, Ensz M, Smugeresky J. Solidification in direct metal deposition by LENS processing. JOM 2001;53:30–4. doi:10.1007/s11837-001-0066-z.

[106] Mahmood K, Stevens N, Pinkerton AJ. Laser surface modification using Inconel 617 machining swarf as coating material. Journal of Materials Processing Technology 2012;212:1271–80. doi:10.1016/j.jmatprotec.2012.01.014.

[107] Jackson MA, Morrow JD, Thoma DJ, Pfefferkorn FE. A comparison of 316 L stainless steel parts manufactured by directed energy deposition using gas-atomized and mechanically-generated feedstock. CIRP Annals - Manufacturing Technology 2020;69:165–8. doi:10.1016/j.cirp.2020.04.042.

[108] Razumov NG, Masaylo D V, Silin AO, Borisov E V, Ozerskoy NE, Goncharov IS, et al. Investigation of additive manufacturing from the heat-resistant steel powder produced by recycling of the machining chips. Journal of Manufacturing Processes 2021;64:1526–6125. doi:10.1016/j.jmapro.2021.02.025.

[109] Nazari KA, Rahman Rashid RA, Palanisamy S, Xia K, Dargusch MS, Rashid RAR, et al. A novel Ti-Fe composite coating deposited using laser cladding of low cost recycled nano-crystalline titanium powder. Materials Letters 2018;229:301–4. doi:10.1016/j.matlet.2018.07.038.

[110] Murray JW, Speidel A, Jackson-Crisp A, Smith PH, Constantin H, Clare AT. Unprocessed machining chips as a practical feedstock in directed energy deposition. International Journal of Machine Tools and Manufacture. 2021; 169:103803.

[111] Fullenwider B, Kiani P, Schoenung JM, Ma K. From recycled machining waste to useful

powders for metal additive manufacturing. Minerals, Metals and Materials Series, Springer International Publishing; 2019, p. 3–7. doi:10.1007/978-3-030-10386-6_1.

[112] The Iron and Steel Statistics Bureau. United Kingdom Iron and Steel Industry Annual Statistics. 2021.

[113] Ingarao G, Amato M, Latif A, La Rosa AD, Di Lorenzo R, Fratini L. Life Cycle Assessment of aluminum alloys chips recycling through single and multi-step Friction Stir Consolidation processes. Journal of Manufacturing Systems. 2023; 68:651-9. doi:10.1016/j.jmsy.2023.05.021.

[114] Duflou JR, Tekkaya AE, Haase M, Welo T, Vanmeensel K, Kellens K, Dewulf W, Paraskevas D. Environmental assessment of solid state recycling routes for aluminium alloys: can solid state processes significantly reduce the environmental impact of aluminium recycling?. CIRP Annals. 2015; 64(1):37-40. doi:10.1016/j.cirp.2015.04.051.

[115] Milford RL, Allwood JM, Cullen JM. Assessing the potential of yield improvements, through process scrap reduction, for energy and CO2 abatement in the steel and aluminium sectors. Resources, Conservation and Recycling 2011;55:1185–95. doi:10.1016/J.RESCONREC.2011.05.021.

[116] Wang T, Müller DB, Graedel TE. Forging the anthropogenic iron cycle. Environmental Science and Technology 2007;41:5120–9. doi:10.1021/es062761t.

[117] International Energy Agency, Steel and Aluminum, Net Zero Emission Guide. 2023.

[118] KRICHNER G. DER ALUMINIUMSCHROTTMARKT IM WANDEL. Girsel 1994.

[119] Cooper DR, Song J, Gerard R. Metal recovery during melting of extruded machining chips. Journal of Cleaner Production 2018;200:282–92. doi:10.1016/j.jclepro.2018.07.246.

[120] IAI (International Aluminium Institute). Aluminium for Future Generations/2007 update. n.d.

[121] Lazzaro G, Atzori C. Recycling of aluminum trimmings by conform process. Light Metals 1992, 1992, p. 1379–84.

[122] Marin E, Zanocco M, Boschetto F, Santini M, Zhu W, Adachi T, et al. Silicon nitride laser cladding: A feasible technique to improve the biological response of zirconia 2020. doi:10.1016/j.matdes.2020.108649.

[123] Zhao Y, Lu M, Fan Z, Mccormick P, Tan Q, Mo N, et al. Microstructures and mechanical properties of wear-resistant titanium oxide coatings deposited on Ti-6Al-4V alloy using laser cladding 2019. doi:10.1016/j.jeurceramsoc.2019.10.037.

[124] Dobatkin S V, Skrotzki W, Rybalchenko O V, Terent'ev VF, Belyakov AN, Prosvirnin D V, et al. Structural changes in metastable austenitic steel during equal channel angular pressing and subsequent cyclic deformation 2018. doi:10.1016/j.msea.2018.03.018.

[125] Tohidlou E, Bertram A. Effect of initial orientation on subgrain formation in nickel single crystals during equal channel angular pressing. Mechanics of Materials 2017;114:30–9. doi:10.1016/j.mechmat.2017.06.006.

[126] Jiang H, Li L, Dong J, Xie X. Microstructure-based hot extrusion process control principles for nickel-base superalloy pipes. Progress in Natural Science: Materials International 2018;28:391–8. doi:10.1016/j.pnsc.2018.04.009.

[127] Liu CZ, Liu F, Huang L, Jiang L. Effect of hot extrusion and heat treatment on microstructure of nickel-base superalloy. Oral Oncology 2014;50:2544–53. doi:10.1016/S1003-6326(14)63381-1.

[128] Unifantowicz P, Oksiuta Z, Olier P, De Carlan Y, Baluc N. Microstructure and mechanical properties of an ODS RAF steel fabricated by hot extrusion or hot isostatic pressing. Fusion Engineering and Design 2011;86:2413–6. doi:10.1016/j.fusengdes.2011.01.022.

[129] Li C, Li S, An D, Xie Z. Microstructure and mechanical properties of spark plasma sintered SiC ceramics aided by B4C. Ceramics International 2020;46:10142–6. doi:10.1016/j.ceramint.2020.01.005.

[130] won Hong J, Jung WK, Choi DH. Effect of porosity and hexagonality on the infrared transmission of spark plasma sintered ZnS ceramics. Ceramics International 2020;46:16285–90. doi:10.1016/j.ceramint.2020.03.185.

[131] Hu L, Peng H, Baker I, Li L, Zhang W, Ngai T. Characterization of high-strength high-nitrogen austenitic stainless steel synthesized from nitrided powders by spark plasma sintering 2019. doi:10.1016/j.matchar.2019.04.005.

[132] Kan Y, Zhang SH, Zhang LW, Cheng M, Song HW, Lu HW. Healing Behavior of Micropores in Powder Metallurgy 316L Stainless Steel during Hot Forging and Heat Treatment. Journal of Iron and Steel Research International 2014;21:862–8. doi:10.1016/S1006-706X(14)60154-0.

[133] Kumar D, Prakash U, Dabhade V V, Laha K, Sakthivel T. High yttria ferritic ODS steels through powder forging 2017. doi:10.1016/j.jnucmat.2016.12.043.

[134] Korbel A, Pieła K, Ostachowski Pawełand Łagoda M, Błaż L, Bochniak W, Pawlyta M. Structural phenomena induced in the course of and post low-temperature KOBO extrusion of AA6013 aluminum alloy 2017. doi:10.1016/j.msea.2017.10.095.

[135] Deng WJ;, Zhang JY;, Liu LW;, He D&, Xia W. SIMULATION ANALYSIS OF A NEW CHIPS RECYCLING PROCESS TERMED FORMING EXTRUSION CUTTING. Int j Simul Model 2017;16:694–706. doi:10.2507/IJSIMM16(4)CO16.

[136] Shen W, Yu L, Liu H, He Y, Zhou Z, Zhang Q. Diffusion welding of powder metallurgy high speed steel by spark plasma sintering 2019. doi:10.1016/j.jmatprotec.2019.116383.

[137] Vishnu P, Raj Mohan R, Krishna Sangeethaa E, Raghuraman S, Venkatraman R. A review on

processing of aluminium and its alloys through Equal Channel Angular Pressing die 2019. doi:10.1016/j.matpr.2019.04.223.

[138] Riveiro A, Mejías A, Lusquiños F, del Val J, Comesaña R, Pardo J, et al. Laser cladding of aluminium on AISI 304 stainless steel with high-power diode lasers. Surface and Coatings Technology 2014;253:214–20. doi:10.1016/j.surfcoat.2014.05.039.

[139] Carruth MA, Allwood JM. A novel process for transforming sheet metal blanks: Ridged die forming n.d. doi:10.1016/j.cirp.2013.03.052.

[140] Cullen JM, Allwood JM, Bambach MD. Mapping the Global Flow of Steel: From Steelmaking to End-Use Goods. Environmental Science & Technology 2012;46:13048–55. doi:10.1021/es302433p.

[141] Majeske KD, Hammett PC. Identifying Sources of Variation in Sheet Metal Stamping *. vol. 15. 2003.

[142] Horton PM, Allwood JM. Yield improvement opportunities for manufacturing automotive sheet metal components. Journal of Materials Processing Technology 2017;249:78–88. doi:10.1016/J.JMATPROTEC.2017.05.037.